Electronic Supporting Information

Asymmetric [N-I-N]$^+$ halonium complexes in solution?

Daniel von der Heiden, Kari Rissanen and Máté Erdélyi

Table of Contents

General information

The solvents CH_2Cl_2 CH_3CN, CD_2Cl_2 and CD_3CN were distilled over CaH_2, and *n*-hexane was distilled over Na, benzophenone and tetraglyme. All dry solvents were then stored over 3 Å molecular sieves in a glovebox. All other chemicals were purchased from commercial suppliers and used without further purification. For all synthesis and analytical studies, the glassware had been dried at 150 °C in an oven, or *in vacuo*, at least overnight. NMR spectra were recorded on a Bruker Avance Neo 500 MHz NMR spectrometer equipped with a TXO cryogenic probe (TXO (CRPHe TR-^{13}C/^{15}N/^{1}H 5mm-Z)), or on an Agilent MR-400 spectrometer equipped with an OneNMR probe. Chemical shifts are reported on the δ scale (ppm), with the residual solvent signal or TMS as an internal reference; CD_2Cl_2 ($δ_H$ 5.32, $δ_C$ 54.00), $CDCl_3$ ($δ_H$ 7.26, $δ_C$ 77.16), TMS ($δ_H$ 0.00, $δ_C$ 0.00). Nitromethane ($δ_N$ 0.0 ppm) was used as an external standard for ^{15}N. To assign the ^{1}H NMR resonances, chemical shift (δ), multiplicity, coupling constants (*J* Hz) and number of hydrogens were considered. 2D spectra (^{1}H-^{15}N HMBC, ^{1}H-^{13}C HSQC, ^{1}H-^{13}C HMBC) were used to aid assignment. Multiplicities are denoted as s (singlet), d (doublet), t (triplet), q (quartet), hep (heptet), and m (multiplet). MestReNova 12.0.3 was used to process the NMR spectra. Mass spectrometric data have been recorded with an expression® CMS (compact mass spectrometer) using an ESI ion source.

All NMR work was performed under inert gas (N_2) and with careful water exclusion. We followed sample stability by recording ^{1}H NMR spectra from $δ = 0$-20 ppm and thus observing potential pyridinium (py$_x$H$^+$) resonances at $δ = 17$–12 ppm, typically formed in I$^+$/H$^+$ substitution reactions, or in decomposition reactions in the presence of H_2O.[1] If the moisture content is high, or if there is decomposition taking place, the pyridinium resonances are often not observable as they are typically coalesced with the signals of free/protonated pyridine. Iodine(I) salts have been stored under inert gas in a −20 °C freezer.

1. Synthesis

a. [Bis(pyridine)iodine(I)]BF$_4$ ([(1)$_2$I])
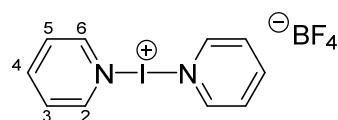
^{1}H NMR (500 MHz, CD_2Cl_2): δ [ppm] = 8.78 (dt, J_{HH} = 5.3, 1.5 Hz, 2H, H–2, H–6), 8.22 (tt, J_{HH} = 7.8, 1.5 Hz, 1H, H–4), 7.63 (m, 2H, H–3, H–5).
^{13}C NMR (126 MHz, CD_2Cl_2): δ [ppm] = 150.0 (C-2, C-6), 142.7 (C-4), 128.5 (C-3, C-5).
^{15}N NMR (51 MHz, CD_2Cl_2): δ [ppm] = −174.

^{1}H NMR (500 MHz, CD_3CN): δ [ppm] = 8.78 (dd, J_{HH} = 6.4, 1.5 Hz, 2H, H–2, H–6), 8.25 (tt, J_{HH} = 7.6, 1.5 Hz, 1H, H–4), 7.63 (m, 2H, H–3, H–5).
^{13}C NMR (126 MHz, CD_3CN): δ [ppm] = 150.6 (C-2, C-6), 143.2 (C-4), 128.8 (C-3, C-5).

8.79
8.79
8.78
8.78
8.77
8.24
8.24
8.23
8.22
8.22
8.21
8.21
7.65
7.64
7.64
7.63
7.63
7.63
7.62
7.62
7.62
5.32
5.32
5.32

| B (tt) |
| 8.22 |
| J(7.78, 1.53) |

A (dt)	C (m)
8.78	7.63
J(5.30, 1.53)	

2.00
0.88
2.12

16 15 14 13 12 11 10 9 8 7 6 5 4 3 2 1 0 -1 -2 -3
f1 (ppm)
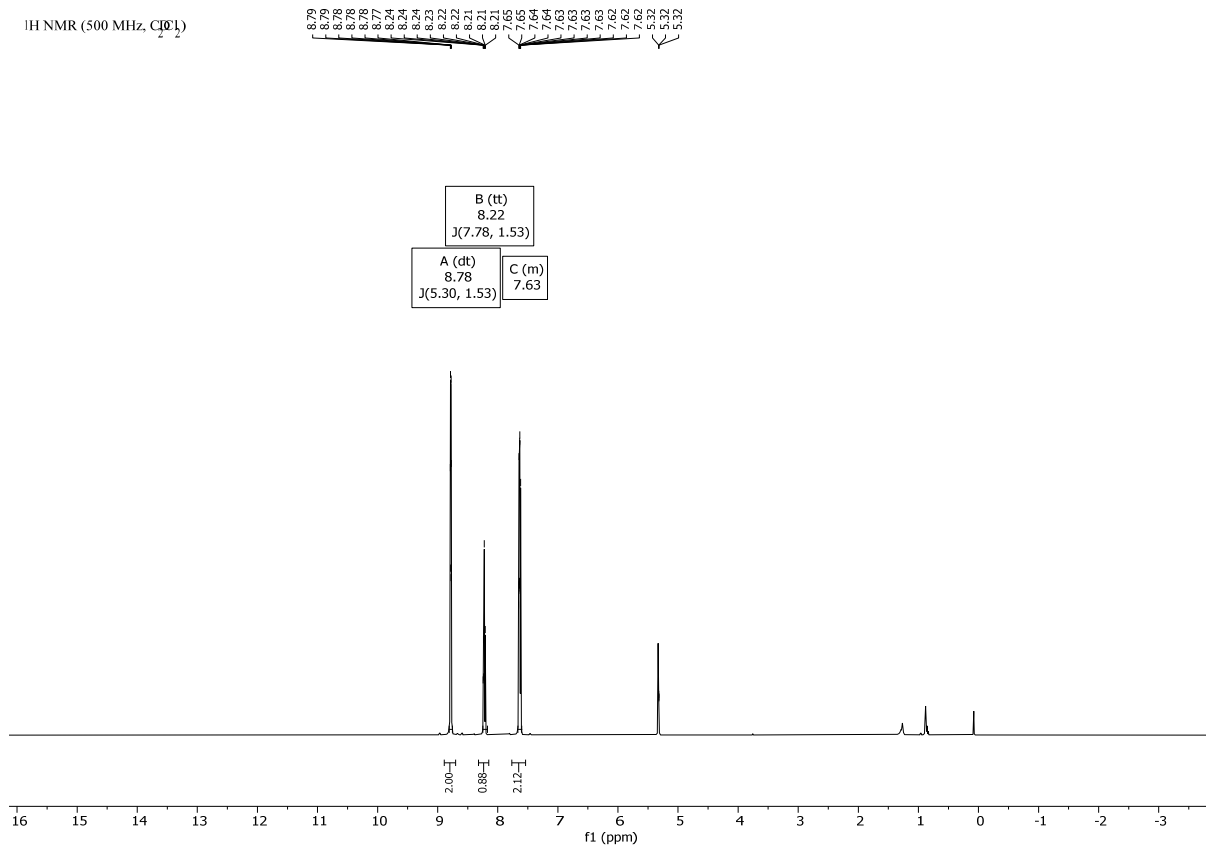
*Figure S1: ^{1}H (500 MHz, CD$_2$Cl$_2$, 298 K) of [bis(pyridine)iodine(I)]BF$_4$ ([(**1**)$_2$I]).*

150.0

142.7

128.5

54.4
54.2
54.0
53.8
53.6

210 200 190 180 170 160 150 140 130 120 110 100 90 80 70 60 50 40 30 20 10 0
f1 (ppm)
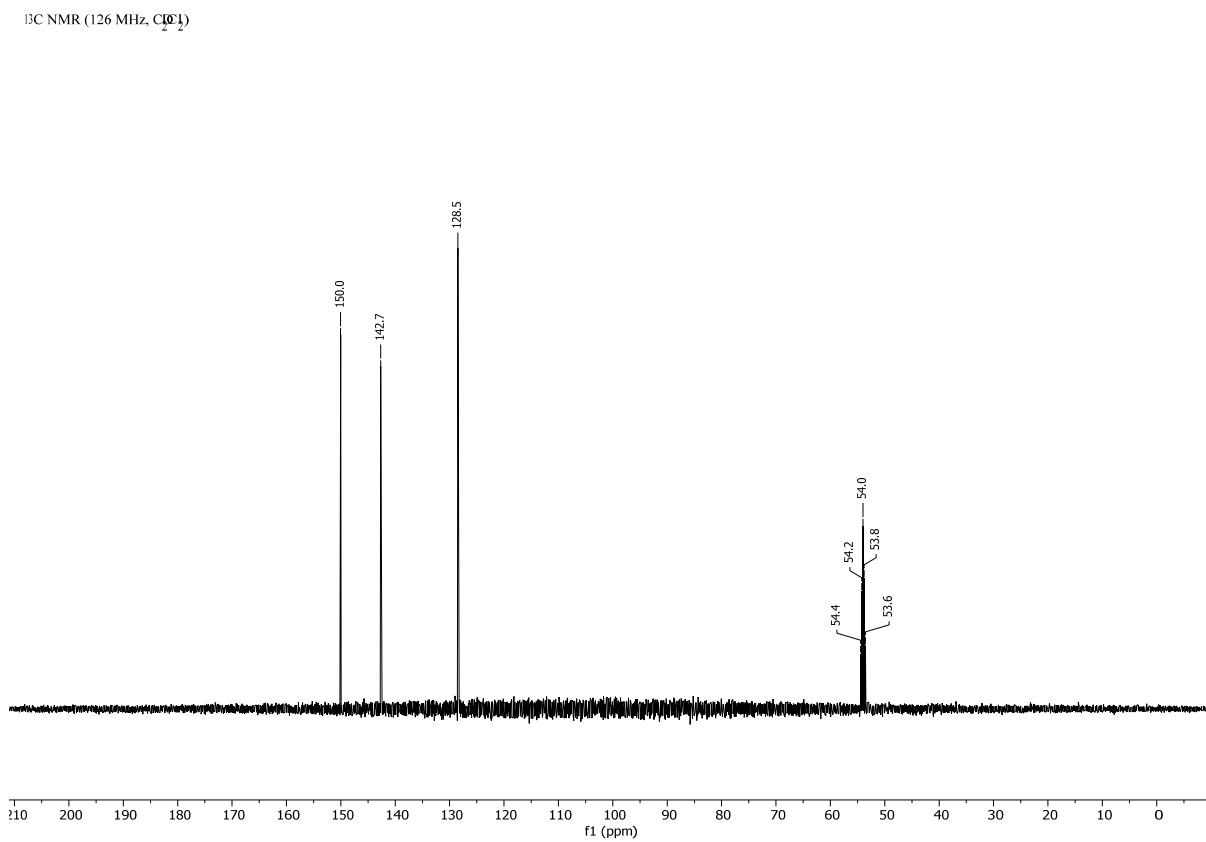
*Figure S2: ^{13}C (126 MHz, CD$_2$Cl$_2$, 298 K) of [bis(pyridine)iodine(I)]BF$_4$ ([(**1**)$_2$I]).*
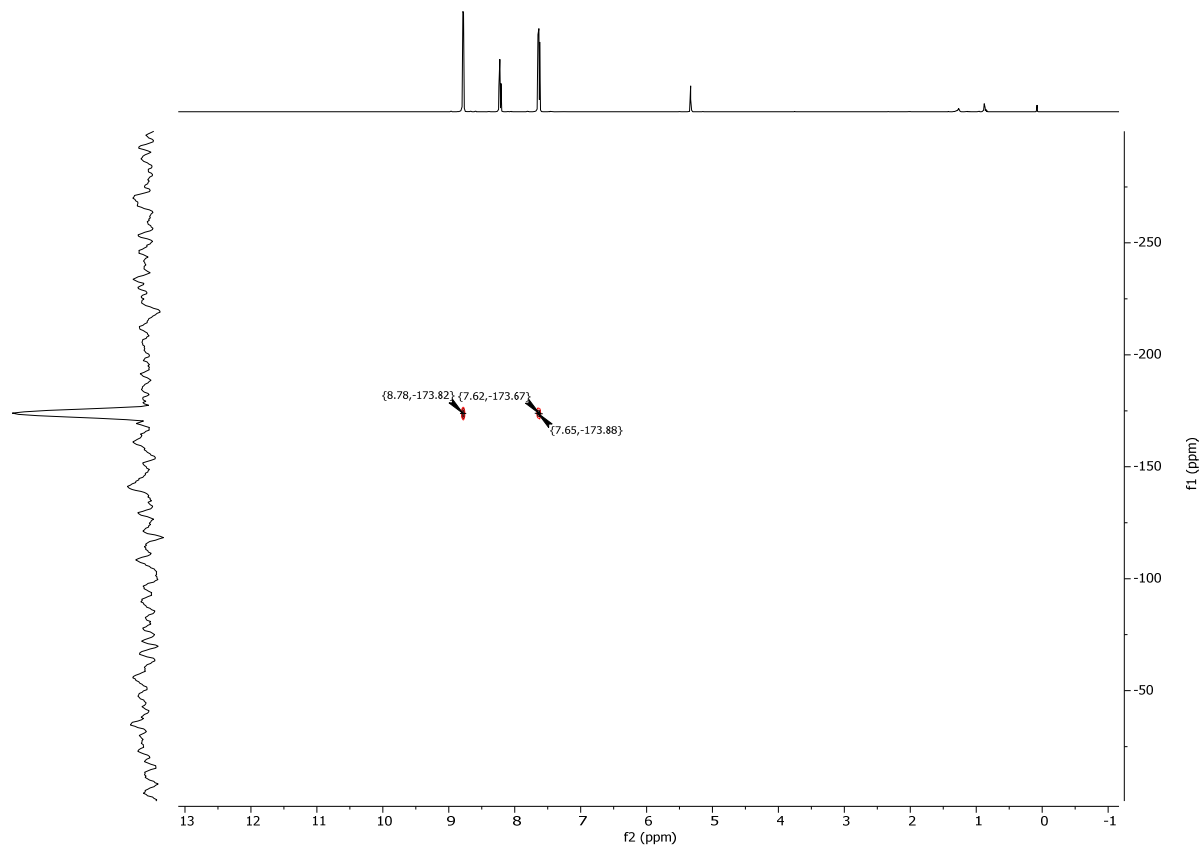
Figure S3: $^1H^{15}N$-HMBC (500/51 MHz, CD_2Cl_2, 298 K) of [bis(pyridine)iodine(I)]BF_4 ([(**1**)$_2$I]).
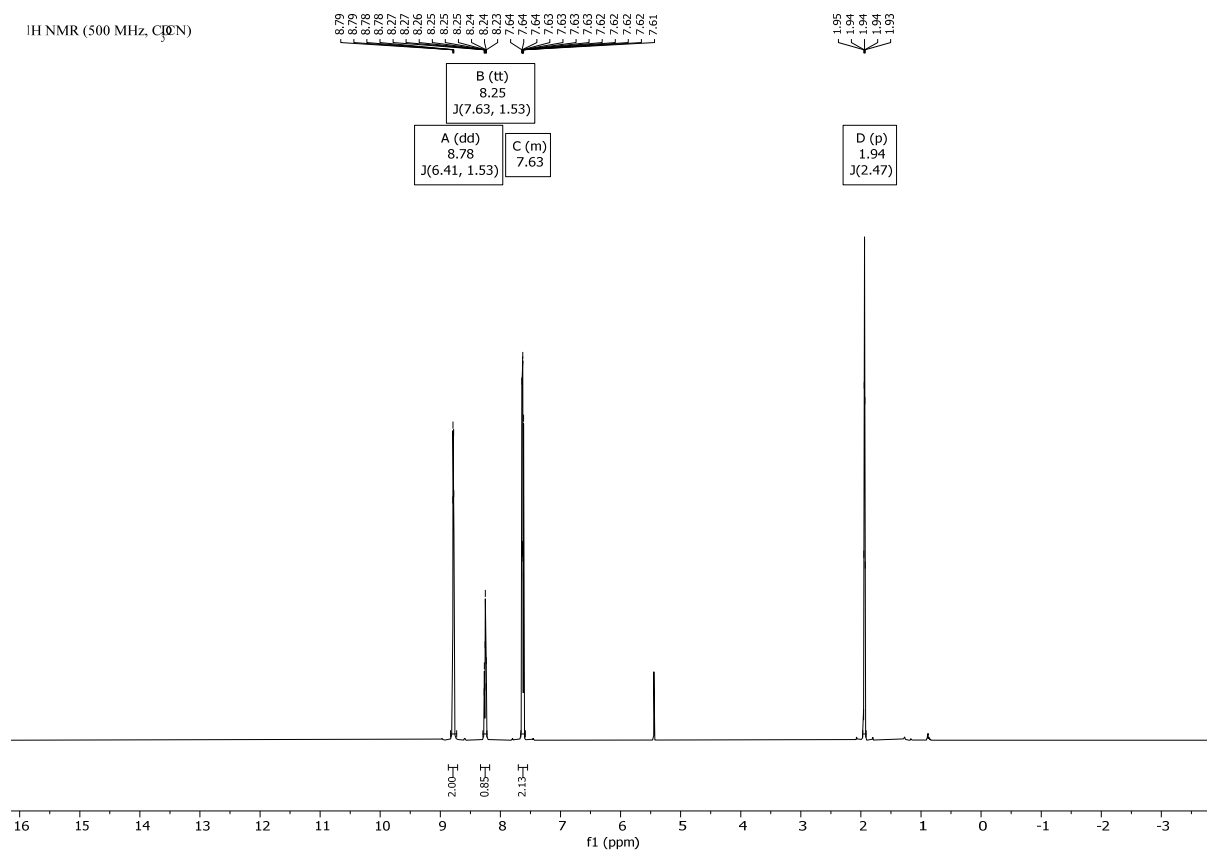
Figure S4: ^1H (500 MHz, CD_3CN, 298 K) of [bis(pyridine)iodine(I)]BF_4 ([(**1**)$_2$I]).

13C NMR (126 MHz, CD3CN)

150.62 143.19 128.80 118.26
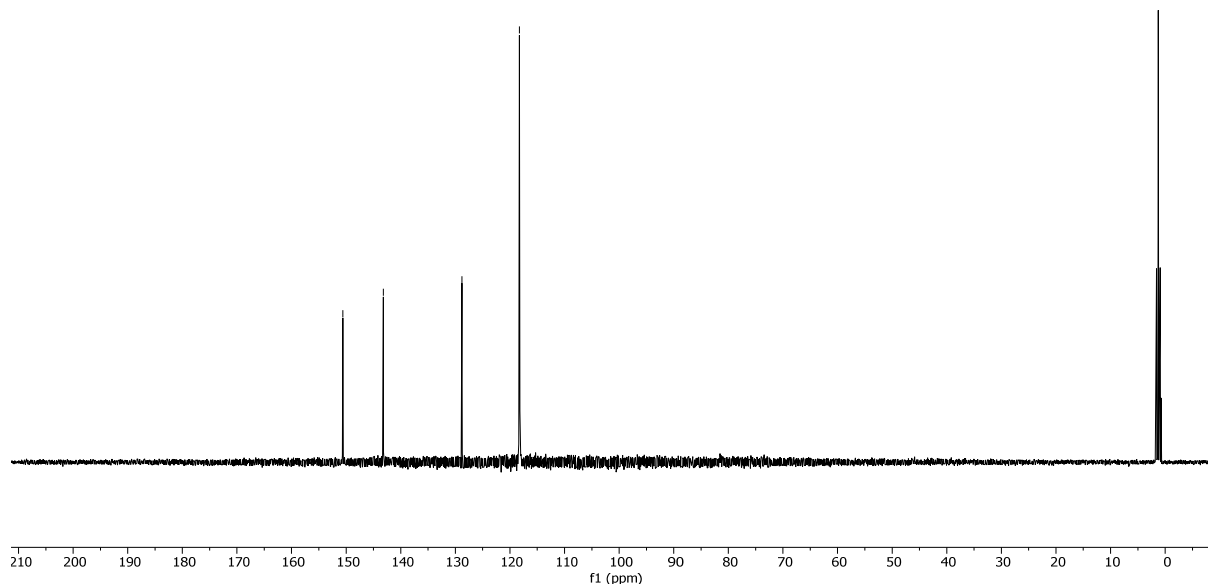
*Figure S5: ^{13}C (126 MHz, CD$_3$CN, 298 K) of [bis(pyridine)iodine(I)]BF$_4$ ([(**1**)$_2$I]).*

b.   [Bis(5,6,7,8-tetrahydroisoquinoline)iodine(I)]BF$_4$ ([(**2**)$_2$I])
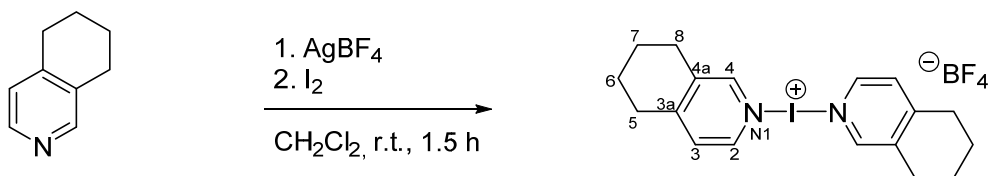
2

To 5,6,7,8-tetrahydroisoquinoline (100 mg, 0.75 mmol, 2.00 eq.) dissolved in CH$_2$Cl$_2$ (2 mL), AgBF$_4$ (73 mg, 0.38 mmol, 1.00 eq.) was added, and the mixture was stirred until all AgBF$_4$ was dissolved (~10 min). Next, iodine (95 mg, 0.38 mmol, 1.00 eq.) was added as a solid, and the mixture was stirred for 1.5 h while yellow AgI precipitate formed. After completion of the reaction, the purple solution was filtered using a PTFE filter and the product was precipitated by dropwise addition of *n*-hexane (4-6 mL). The precipitate was washed twice with *n*-hexane, and solvent residues were removed in vacuum. The product [bis(2-fluoropyridine)iodine(I)] BF$_4$ (140 mg, 0.29 mmol, 39 %) was stored at −20°C.

^{1}H NMR (400 MHz, CD$_2$Cl$_2$): δ [ppm] = 8.37 (s, 1H, H–4), 8.34 (dd, J_{HH} = 5.8, 0.8 Hz, 1H, H–2), 7.22 (d, J_{HH} = 5.9 Hz, 1H, H–3), 2.90–2.80 (m, 4H, 5–H, 8–H), 1.89–1.82 (m, 4H, 6–H, 7–H).
^{13}C NMR (101 MHz, CD$_2$Cl$_2$): δ [ppm] = 149.4 & 145.8 (C-2, C-8), 128.3 (C-3), 29.7 (C-5), 26.8 (C-6), 22.0 & 21.9 (C-6, C-7).

IH NMR (400 MHz, CD₂Cl₂)

8.37
8.34
8.34
8.33
8.33

7.23
7.22

5.32
5.32
5.32

2.89
2.83

1.87
1.86
1.86
1.86
1.85
1.84

| 2 (dd) |
| 8.34 |
| J(5.77, 0.79) |

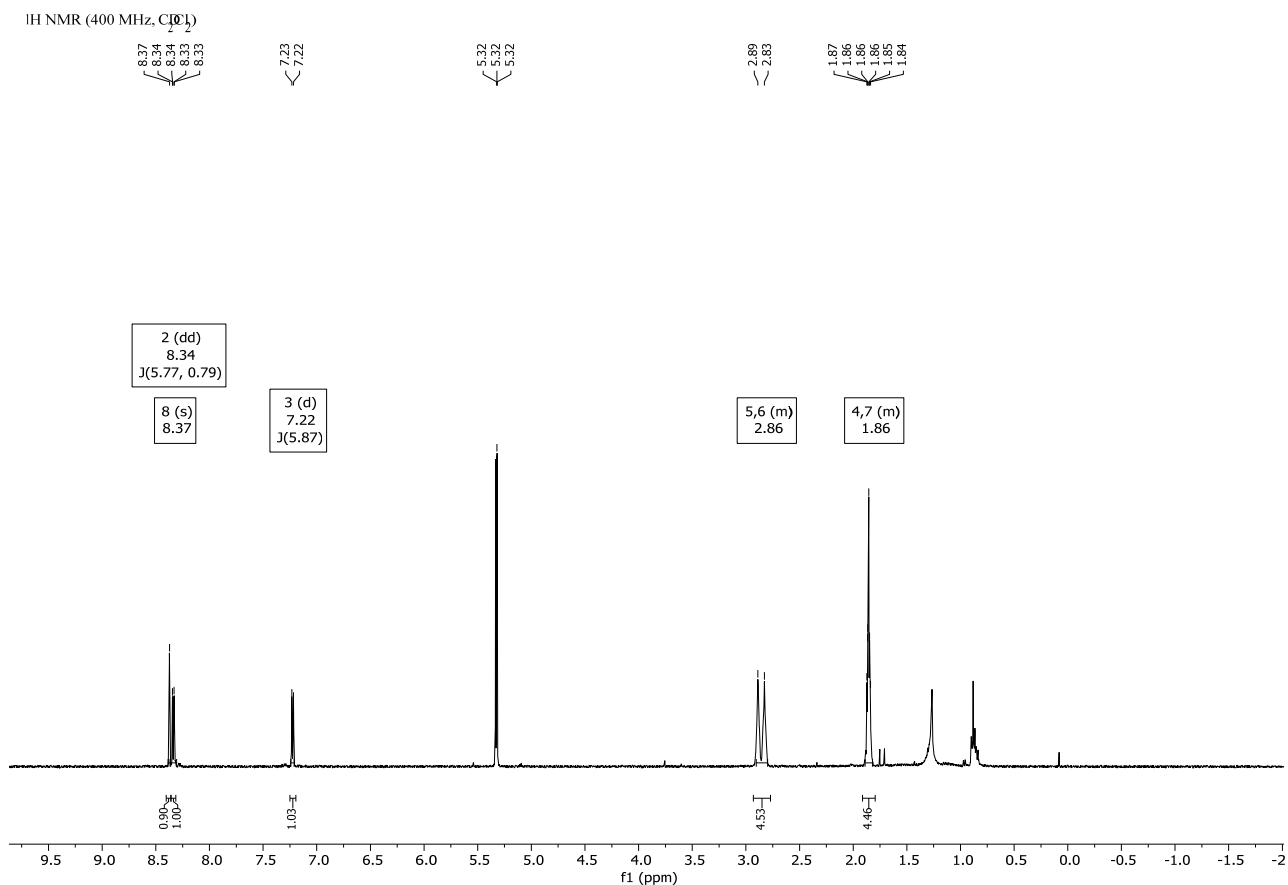| 8 (s) | | 3 (d) | | 5,6 (m) | | 4,7 (m) |
| 8.37 | | 7.22 | | 2.86 | | 1.86 |
| | | J(5.87) | | | | |

Figure S6: ¹H (400 MHz, CD₂Cl₂, 298 K) of [bis(5,6,7,8-tetrahydroisoquinoline)iodine(I)]BF₄ ([(**2**)₂I]).

I3C NMR (101 MHz, CD₂Cl₂)

149.35
145.85

128.29
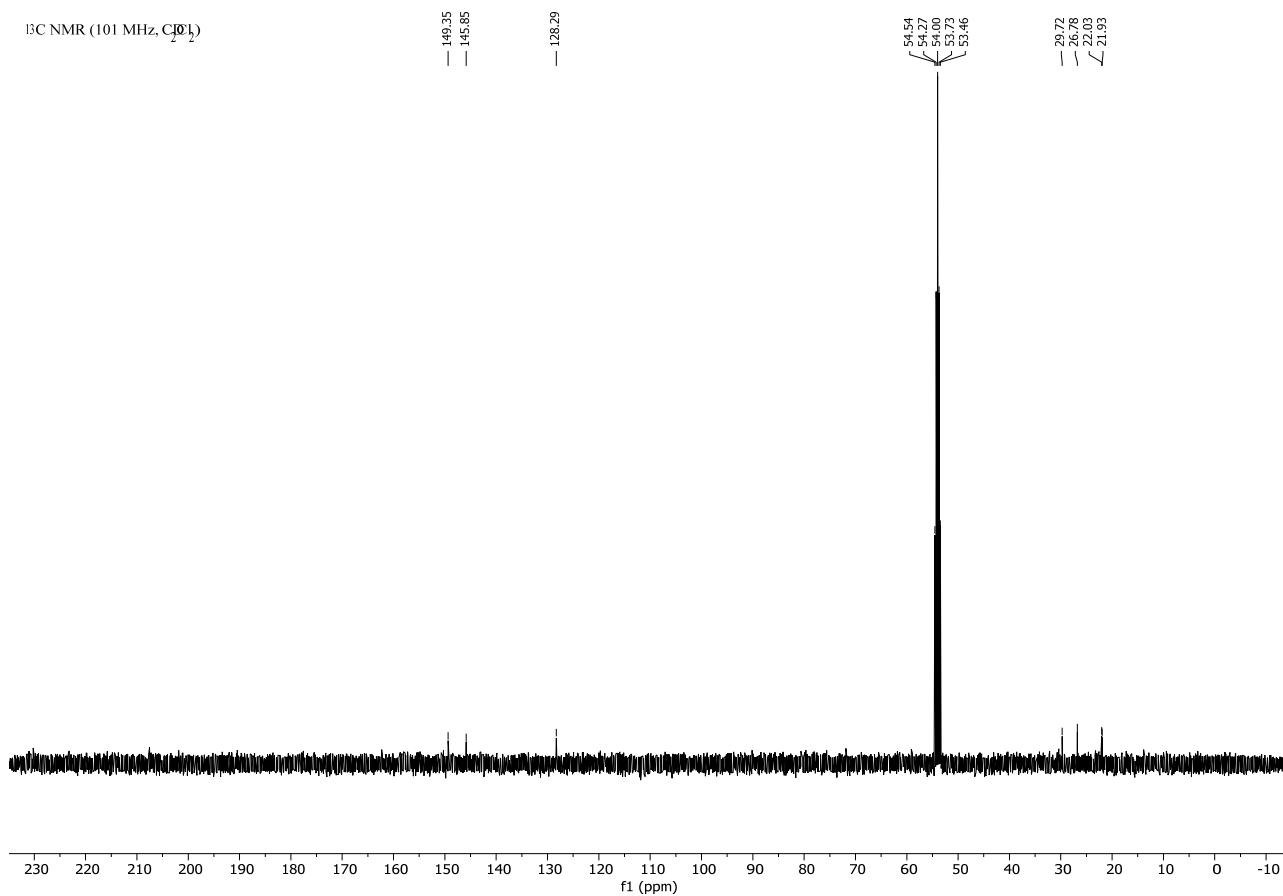
54.54
54.27
54.00
53.73
53.46

29.72
26.78
22.03
21.93

*Figure S7: ¹³C (101 MHz, CD₂Cl₂, 298 K) of [bis(5,6,7,8-tetrahydroisoquinoline)iodine(I)]BF₄ ([(**2**)₂I]).*

c. [Bis(2-fluoropyridine)iodine(I)]BF$_4$ ([(3)$_2$I])
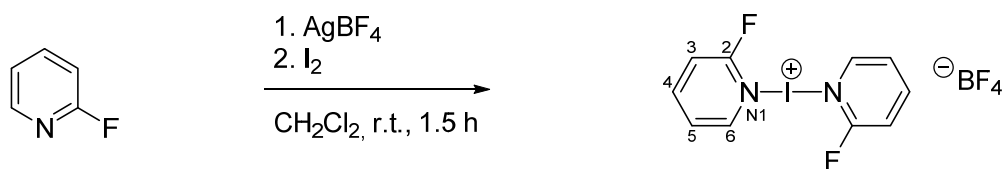
3

2-Fluoropyridine (100 mg, 1.03 mmol, 2.00 eq.) was dissolved in CH$_2$Cl$_2$ (2 mL), AgBF$_4$ (100 mg, 0.51 mmol, 1.00 eq.) was added and the mixture was stirred until all AgBF$_4$ has been dissolved (~10 min). Next Iodine (140 mg, 0.55 mmol, 1.07 eq.) was added as a solid and the mixture was stirred for 1.5 h while a yellow AgI precipitate formed. After completion of the reaction, the purple solution was filtered using a PTFE filter and the product was precipitated by dropwise addition of *n*-hexane (4-6 mL). The precipitate was washed twice with *n*-hexane and then all solvent residues were removed in vacuum. The product [bis(2-fluoropyridine)iodine(I)]BF$_4$ (137 mg, 0.33 mmol, 65 %) was stored at −20°C.

^{1}H NMR (500 MHz, CD$_3$CN): δ [ppm] = 8.59 (br., 1H, H–4), 8.33 (br., 1H, H–6), 7.45 (m, 2H, H–3, H–5).
^{13}C NMR (125 MHz, CD$_3$CN): δ [ppm] = 164.4 (d, $^1J_{CF}$ = 114.1 Hz, C-2), 149.7 (br., C-4), 149.3 (br., C-6), 125.4 (br., C-5), 113.6 (br., C-3).

*Figure S8: ^{1}H (500 MHz, CD$_3$CN, 298 K) of [Bis(2-fluoropyridine)iodine(I)]BF$_4$ ([(**3**)$_2$I]).*

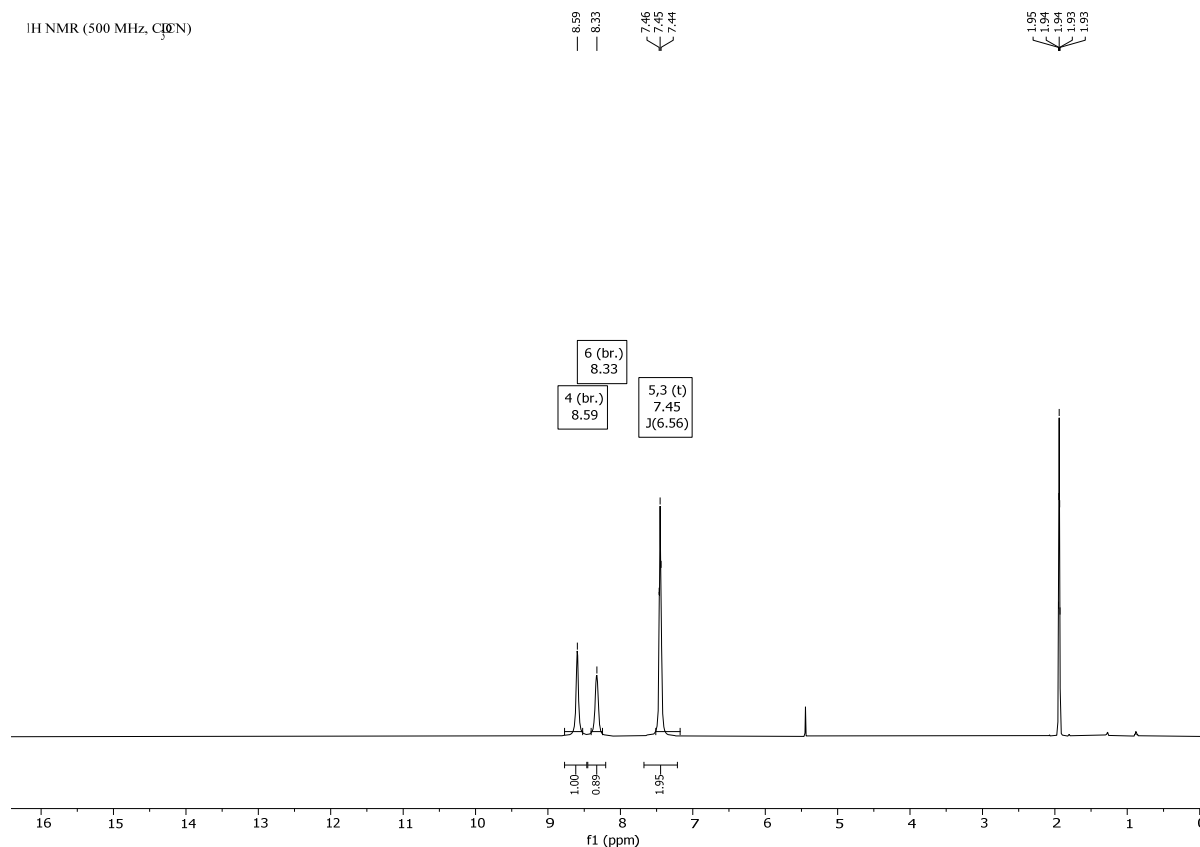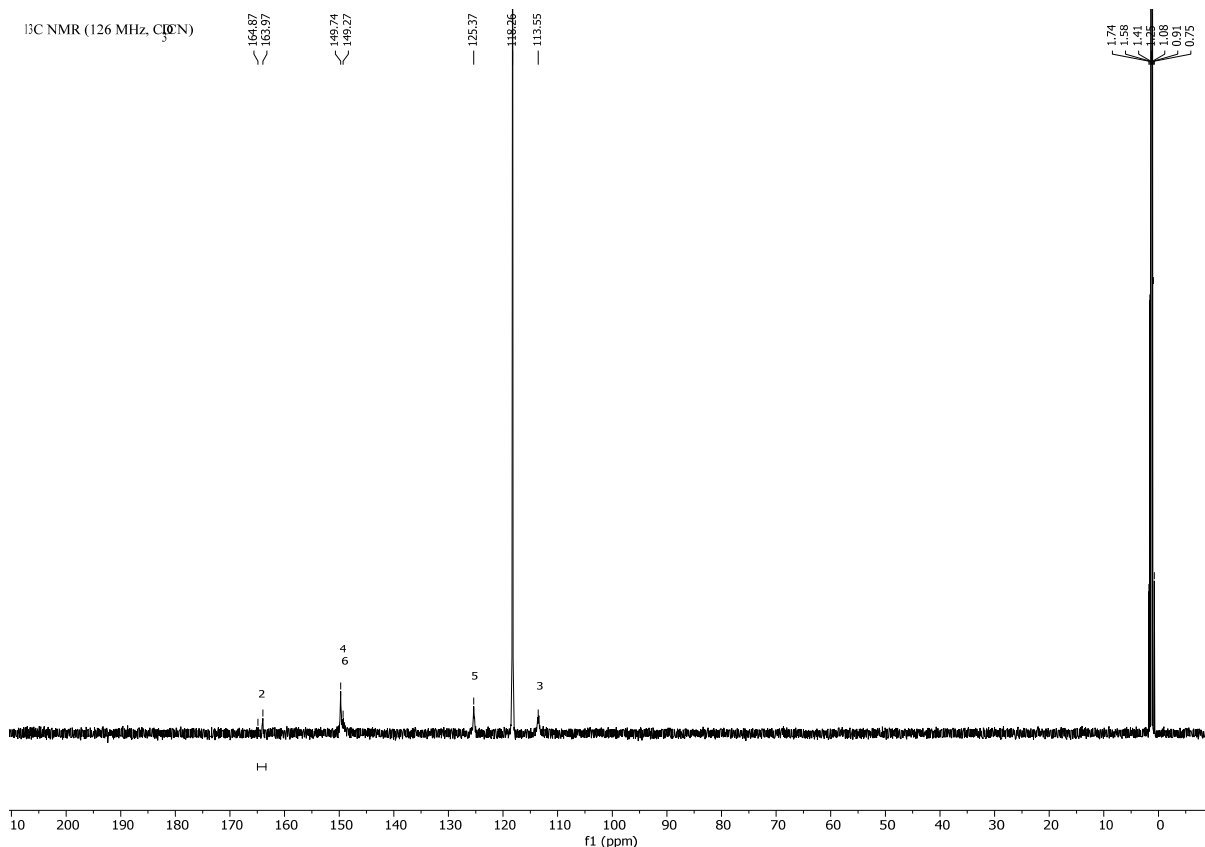*Figure S9: ^{13}C (125 MHz, CD$_3$CN, 298 K) of [Bis(2-fluoropyridine)iodine(I)]BF$_4$ ([(**3**)$_2$I]).*

d. [Bis(4-(trifluoromethyl)pyridine)iodine(I)]BF$_4$ ([(4)$_2$I])

4-(Trifluoromethyl)pyridine (147 mg, 1.00 mmol, 2.00 eq.) was dissolved in CH$_2$Cl$_2$ (2 mL), AgBF$_4$ (97 mg, 0.50 mmol, 1.00 eq.) was added and the mixture was stirred until all AgBF$_4$ was dissolved (~10 min). Next, Iodine (152 mg, 0.60 mmol, 1.20 eq.) was added as a solid and the mixture was stirred for 1.5 h while yellow AgI precipitate was formed. After completion of the reaction, the purple solution was filtered using a PTFE filter, and the product was precipitated by dropwise addition of *n*-hexane (4-6 mL). The precipitate was washed twice with *n*-hexane, and all solvent residues were removed in vacuum. The product [Bis(4-(trifluoromethyl)pyridine)iodine(I)]BF$_4$ (183 mg, 0.359 mmol, 72 %) was stored at −20°C.[2]

^{1}H NMR (500 MHz, CD$_2$Cl$_2$): δ [ppm] = 9.08 (d, J_{HH} = 6.87 Hz, 2H, H–2, H–6), 7.87 (d, J_{HH} = 6.87 Hz, 2H, H–3, H–5).
^{1}H NMR (500 MHz, CD$_3$CN): δ [ppm] = 9.04 (m, 2H, H–2, H–6), 7.93 (m, 2H, H–3, H–5).
^{13}C NMR (100 MHz, CD$_3$CN): δ [ppm] = 152.8 (br., C-2, C-6), 125.2 (br., C-3, C-5).
^{15}N NMR (51 MHz, CD$_2$Cl$_2$): δ [ppm] = −167.
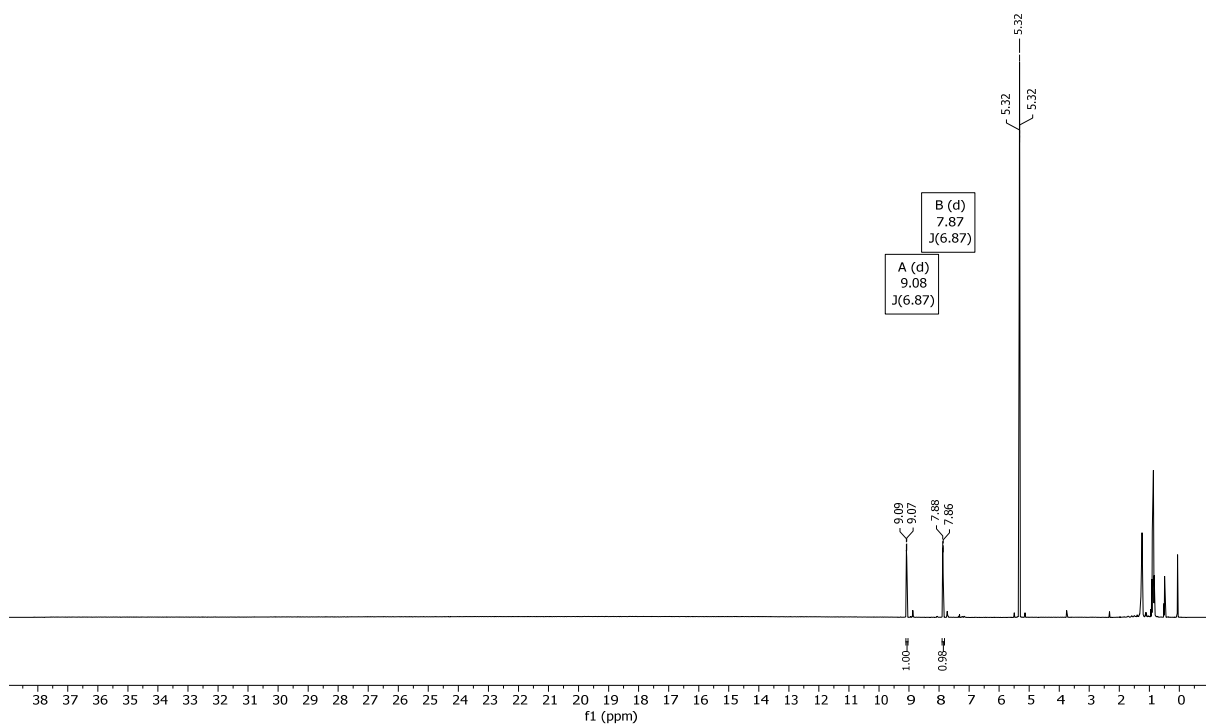
Figure S10: *¹H (500 MHz, CD₂Cl₂, 298 K) of [bis(4-(trifluoromethyl)pyridine)iodine(I)]BF₄ ([(**4**)₂I]).*
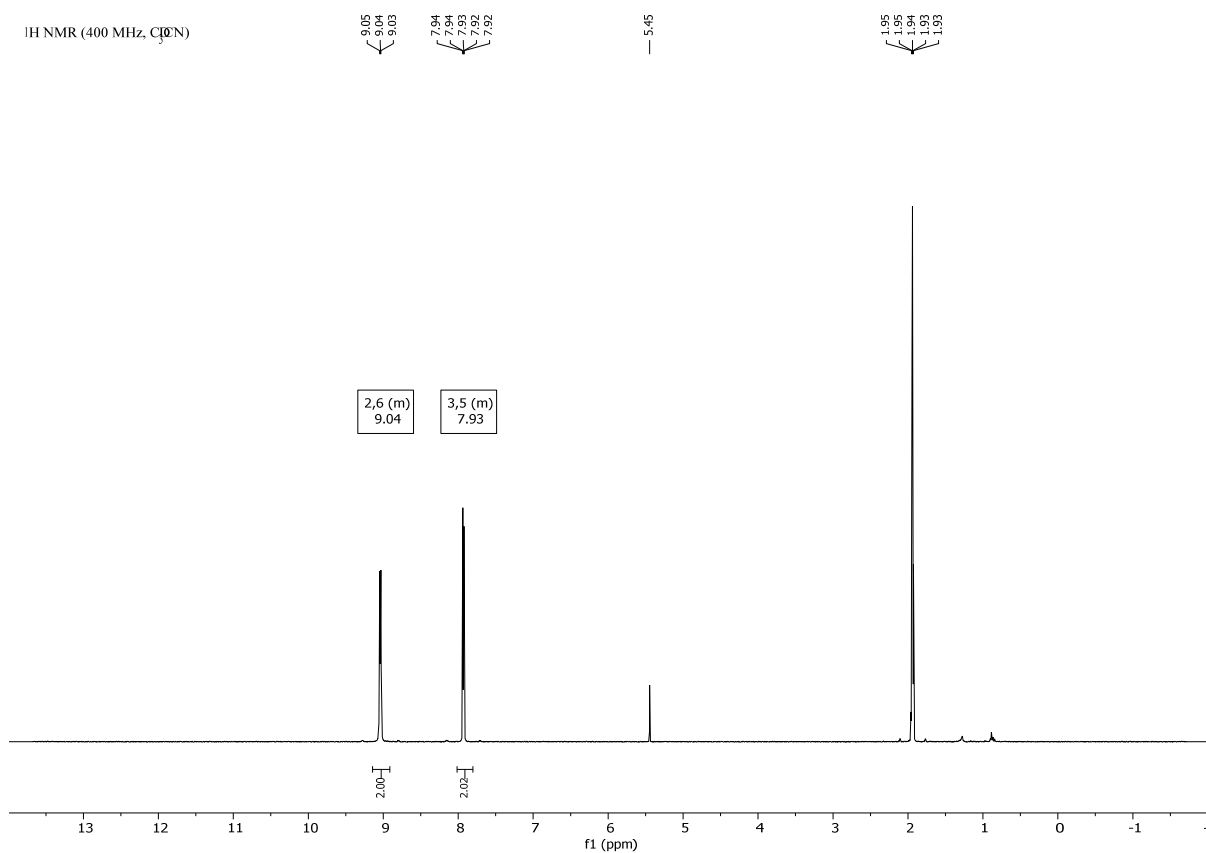
Figure S11: *¹H (500 MHz, CD₃CN, 298 K) of [bis(4-(trifluoromethyl)pyridine)iodine(I)]BF₄ ([(**4**)₂I]).*

152.78

125.19

118.26

230 220 210 200 190 180 170 160 150 140 130 120 110 100 90 80 70 60 50 40 30 20 10 0 -10
f1 (ppm)
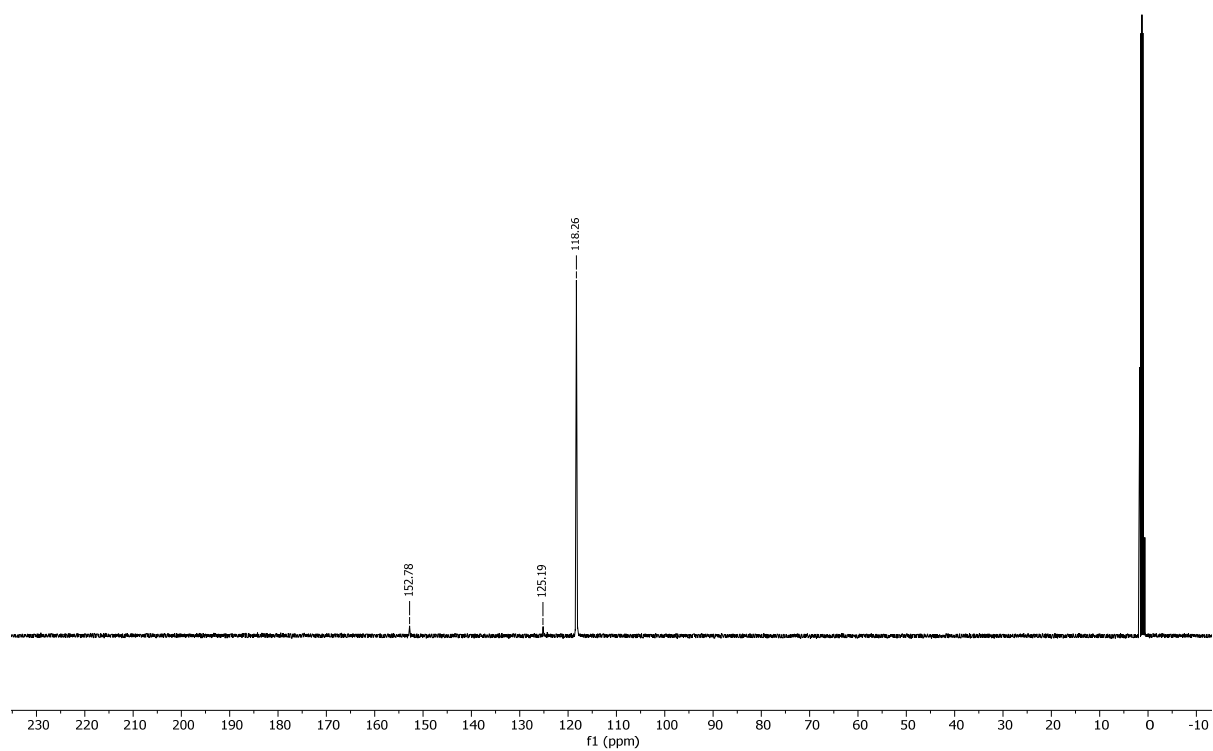
*Figure S12: ^{13}C (100 MHz, CD$_3$CN, 298 K) of [bis(4-(trifluoromethyl)pyridine)iodine(I)]BF$_4$ ([(**4**)$_2$I]).*

{9.11,-166.51}   {7.90,-166.73}

-250

-200

-150

f1 (ppm)

-100

-50

11.5 11.0 10.5 10.0 9.5 9.0 8.5 8.0 7.5 7.0 6.5 6.0 5.5 5.0 4.5 4.0 3.5 3.0 2.5 2.0 1.5 1.0 0.5
f2 (ppm)
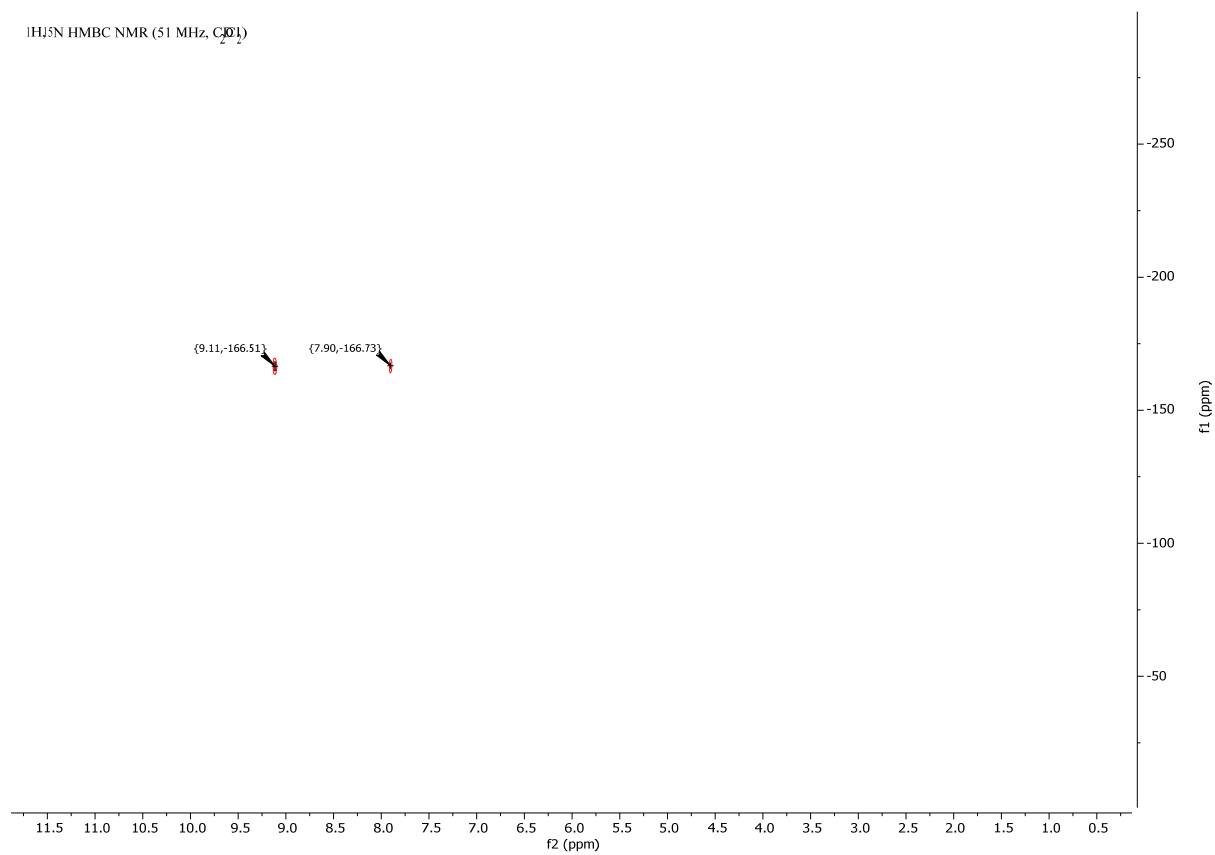
*Figure S13: ^{1}H^{15}N HMBC (500 MHz/51 MHz, CD$_2$Cl$_2$, 298 K) of [bis(4-(trifluoromethyl)pyridine)iodine(I)]BF$_4$ ([(**4**)$_2$I]).*

e.   [Bis(4-(trifluoromethyl)pyridine)iodine(I)]BF$_4$ ([(5)$_2$I])

5

4-(Ethyl)pyridine (250 mg, 265 μL 2.33 mmol, 2.00 eq.) was dissolved in CH$_2$Cl$_2$ (2 mL), AgBF$_4$ (227 mg, 1.17 mmol, 1.00 eq.) was added and the mixture was stirred until all AgBF$_4$ was dissolved (~10 min). Next, Iodine (355 mg, 1.40 mmol, 1.20 eq.) was added as a solid and the mixture was stirred for 1.5 h while a yellow AgI precipitate was formed. After completion of the reaction, the purple solution was filtered using a PTFE filter, and the product was precipitated by dropwise addition of *n*-hexane (10 mL). The precipitate was washed twice with *n*-hexane, and all solvent residues were removed in vacuum. The product [Bis(4-(ethyl)pyridine)iodine(I)]BF$_4$ (413 mg, 0.96 mmol, 82 %) was stored at − 20°C.[3]

^{1}H NMR (500 MHz, CD$_2$Cl$_2$): δ [ppm] = 8.61 − 8.59 (AA'BB', 2H, H-2, H-6), 7.43 − 7.40 (AA'BB', 2H, H-3, H-5), 2.82 (q, J_{HH} = 7.6 Hz, 2H, H-7), 1.29 (t, J_{HH} = 7.6 Hz, 3H, H-8).
^{13}C NMR (125 MHz, CD$_2$Cl$_2$): δ [ppm] = 161.3 (C-4), 149.4 (C-2, C-6), 127.9 (C3, C-5), 29.2 (C-7), 14.0 (C-8).
^{15}N NMR (51 MHz, CD$_2$Cl$_2$): δ [ppm] = −181.
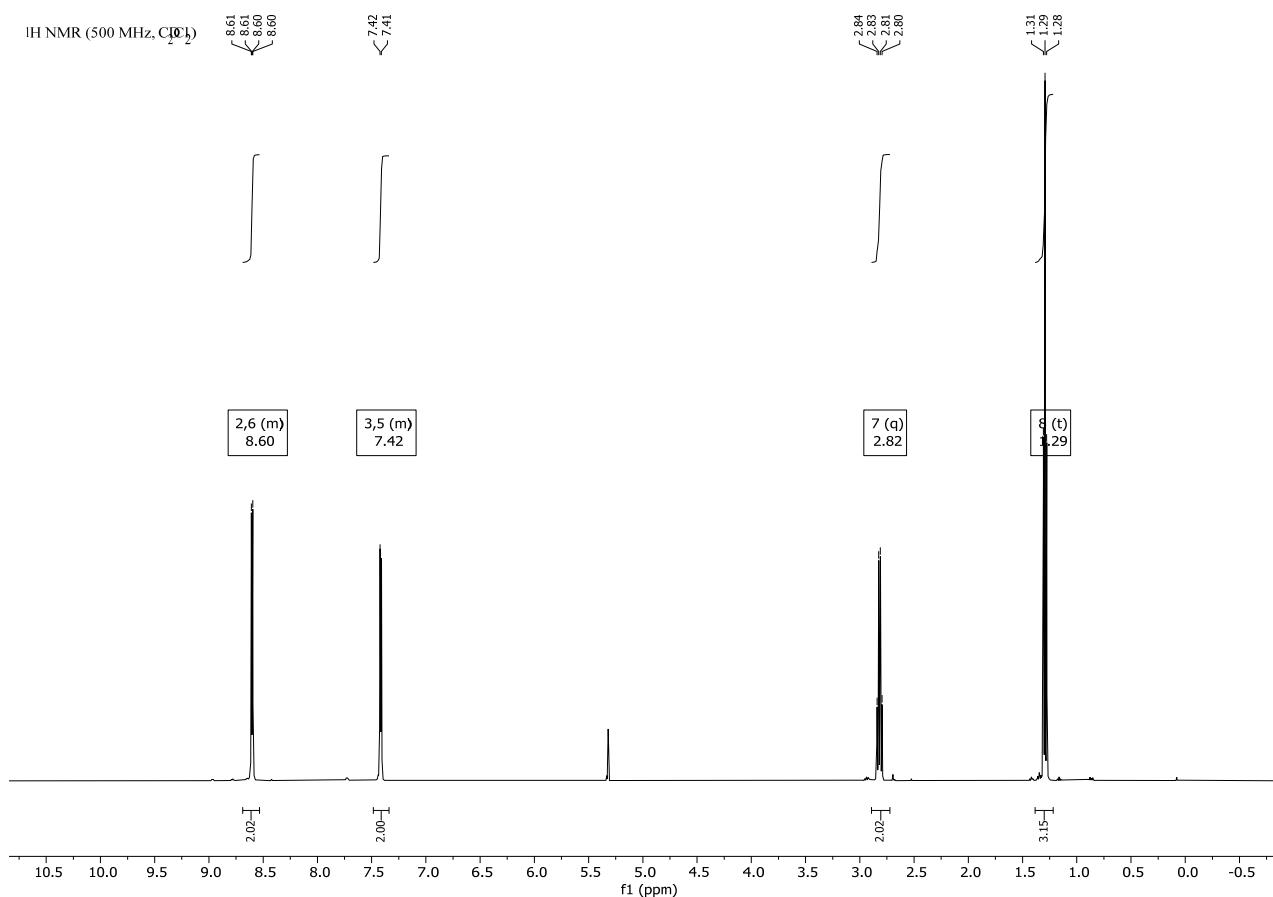
Figure S14: ^{1}H (500 MHz, CD$_2$Cl$_2$, 298 K) of [bis(4-(ethyl)pyridine)iodine(I)]BF$_4$ ([(5)$_2$I]).
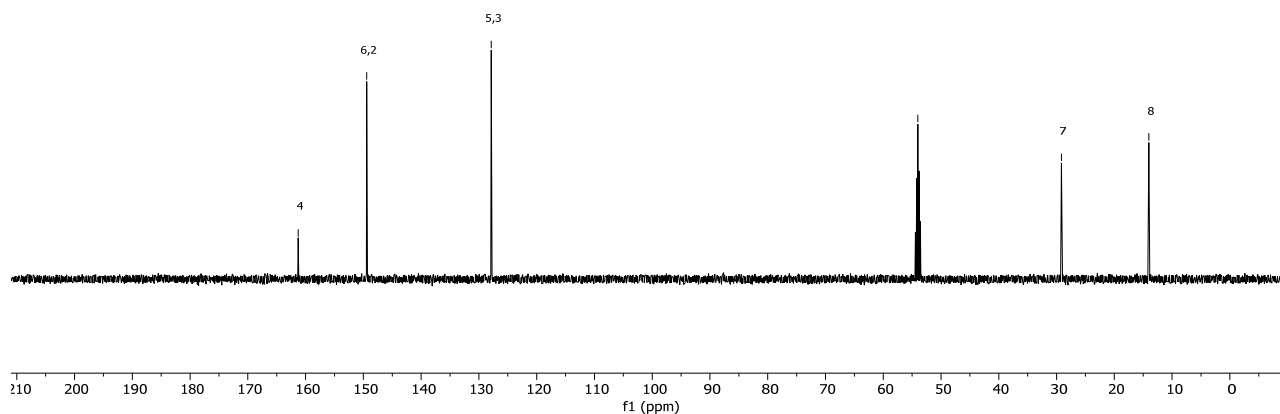
Figure S15: ^{13}C (125 MHz, CD$_2$Cl$_2$, 298 K) of [bis(4-(ethyl)pyridine)iodine(I)]BF$_4$ ([(**5**)$_2$I]).
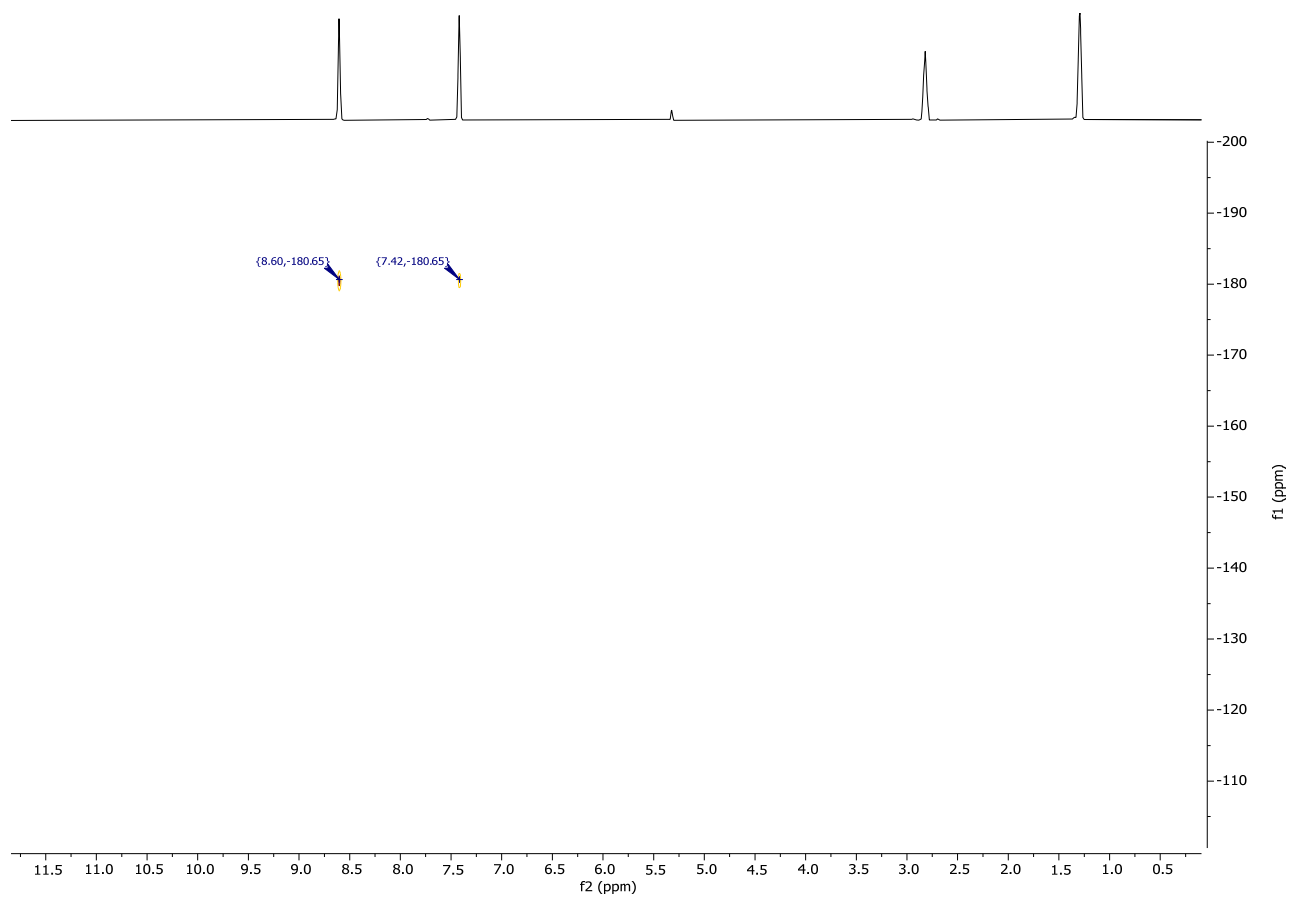
Figure S16: $^1H^{15}N$ HMBC (500 MHz/51 MHz, CD$_2$Cl$_2$, 298 K) of [bis(4-(ethyl)pyridine)iodine(I)]BF$_4$ ([(**5**)$_2$I]).

2. The dynamics of symmetric [bis(pyridine)iodine(I)]⁺-type complexes

a. [Bis(5,6,7,8-tetrahydroisoquinoline)iodine(I)]BF₄ ([(2)₂I])

Mixing [bis(5,6,7,8-tetrahydroisoquinoline)iodine(I)]BF₄ (10 mg, 0.021 mmol, 1.0 eq.) dissolved in dry CD₂Cl₂ with 5,6,7,8-tetrahydroisoquinoline (5.3 μL, 5.5 mg, 0.41 mmol, 2.0 eq.) resulted in a clear colourless solution. The ¹H NMR spectrum of this mixture was measured and compared with the ¹H NMR spectra of the pure constituents. In addition, 1D NOESY spectra (mixing time 200 ms) were recorded to investigate possible ligand exchange process.
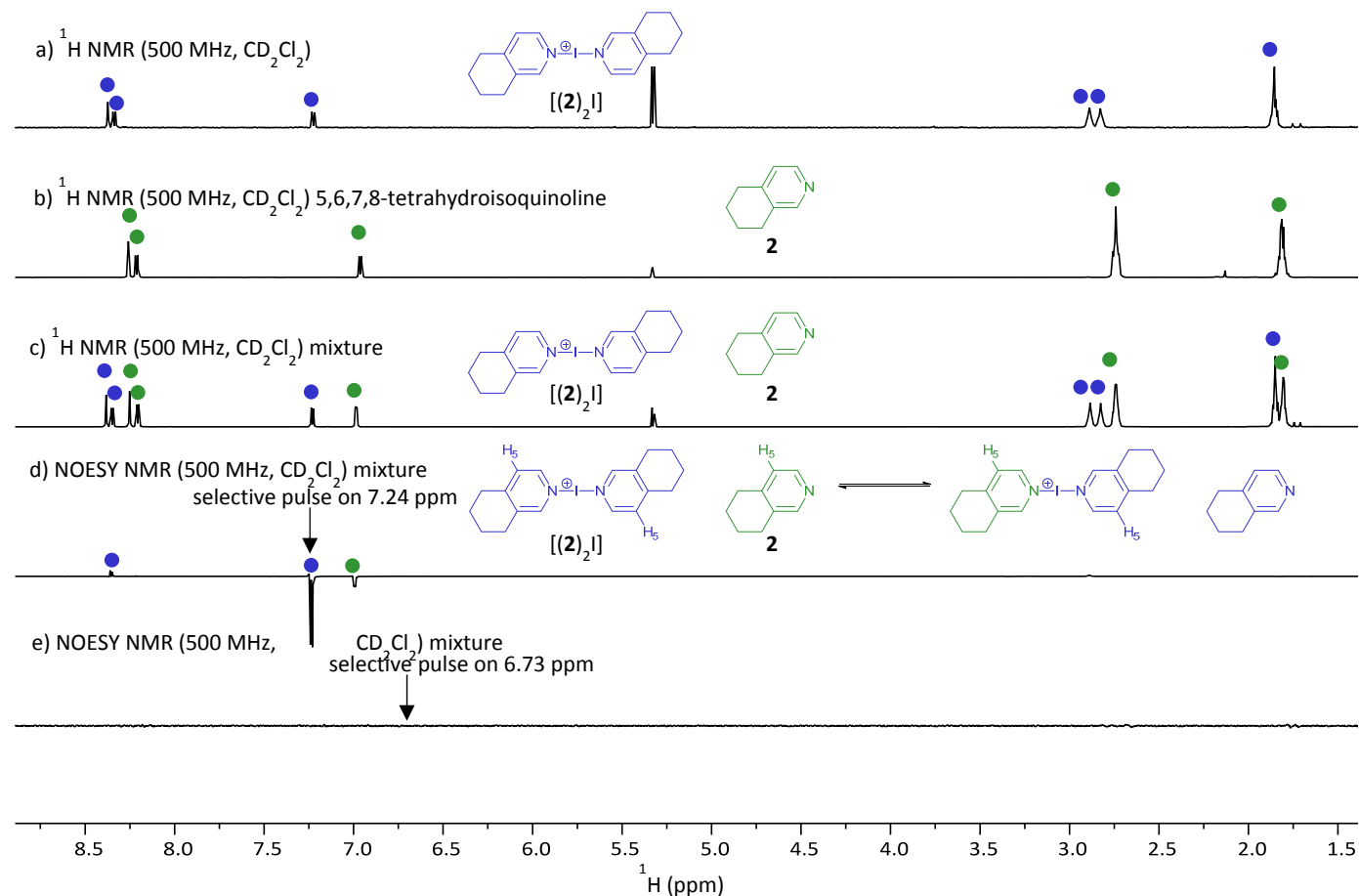
Figure S17: a) ¹H (500 MHz, CD₂Cl₂, 298 K) of a) [bis(5,6,7,8-tetrahydroisoquinoline)iodine(I)]BF₄ ([(2)₂I]); b) of 5,6,7,8-tetrahydroisoquinoline (2); c) 1:2 mixture of [(2)₂I] and 2; d) selective ¹H NOESY of the mixture, with a selective pulse at 7.24 ppm; e) selective ¹H NOESY of the mixture with a selective pulse at 6.73 ppm.

b. [Bis(2-fluoropyridine)iodine(I)]BF$_4$ ([(3)$_2$I])

Mixing [bis(2-fluoropyridine)iodine(I)]BF$_4$ (10 mg, 0.024 mmol, 1.0 eq.) with 2-fluoropyridine (2.1 µL, 2.4 mg, 0.24 mmol, 1.0 eq.) in dry CD$_3$CN resulted in a clear colourless solution. The ^{1}H NMR spectrum of this mixture was measured, and compared with the ^{1}H NMR spectra of the pure constituents.
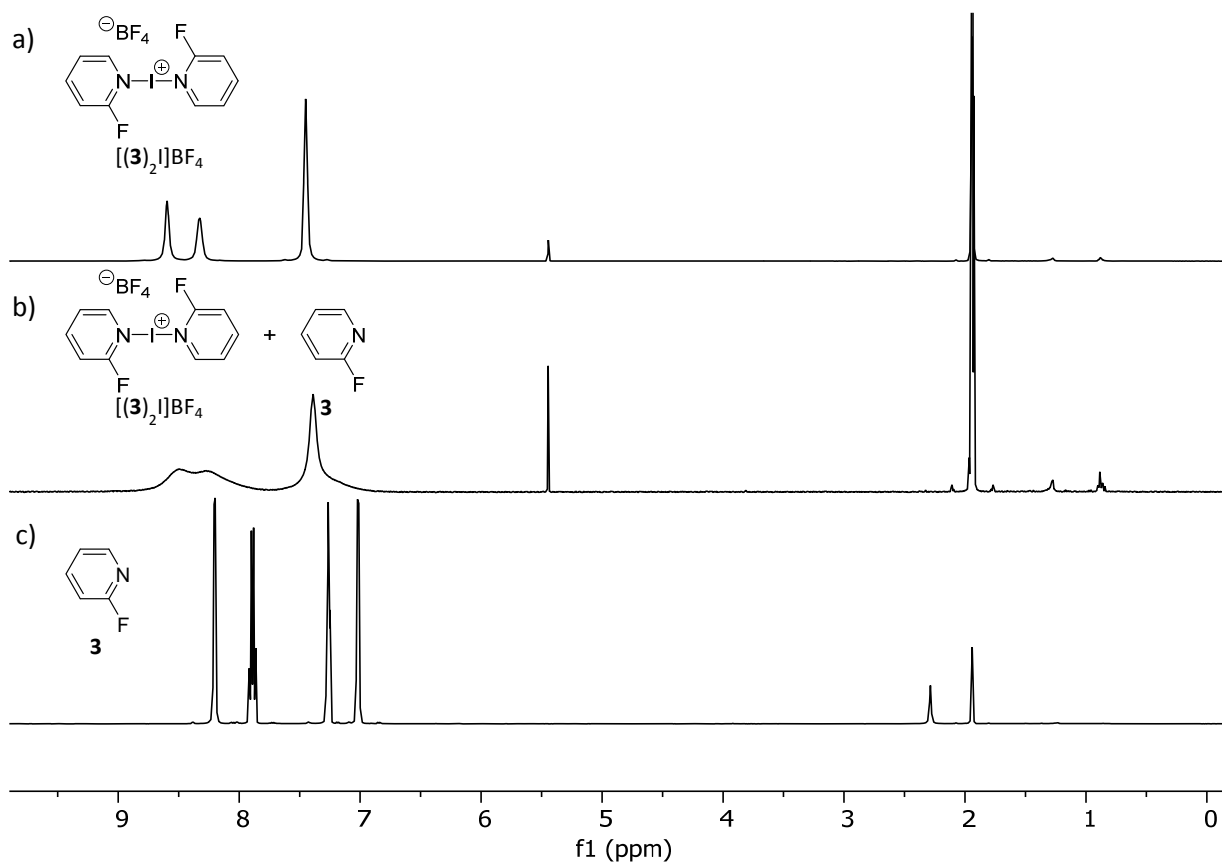
Figure S18: ^{1}H (500 MHz, CD$_3$CN, 298 K) of [bis(2-fluoropyridine)iodine(I)]BF$_4$ (top), a 1:1 mixture of [bis(2-fluoropyridine)iodine(I)]BF$_4$ and 2-fluoropyridine (middle) and pure 2-fluoropyridine (bottom).

c.   Considerations regarding signal coalescence

Based on the most deshielded resonances belonging to H-6 of the pyridines, we compare the hypothetical coalescence conditions of [(**2**)$_2$I] in exchange with **2** and [(**3**)$_2$I] in exchange with **3**, at room temperature and at the same spectrometer frequency, following well-established equations.[4]

$$k(T) = \frac{\pi \Delta v_{AB}}{\sqrt{2}} \approx 2.22 \, \Delta v_{AB}$$

$$k([(\mathbf{2})_2 I]BF_4 - \mathbf{2}, 298 \, K) \approx 2.22 \, \Delta v_{AB} = 2.22 \times 65 Hz = 144.3 \, Hz$$

$$k([(\mathbf{3})_2 I]BF_4 - \mathbf{3}, 298 \, K) \approx 2.22 \, \Delta v_{AB} = 2.22 \times 150 Hz = 333 \, Hz$$

Based on the coalesced proton signals of the mixture of [(**3**)$_2$I] with **3** whereas an absence of coalescence for that of [(**2**)$_2$I] and **2**, a higher ligand exchange rate in the former as compared to the latter mixture is concluded. It is important to note that the look of the spectrum, that is coalescence or not, does not allow one to draw conclusion on the absence or presence of ligand exchange. Line broadening and coalescence is observed upon rapid ligand exchange, for the complexes of weak halogen bond acceptor (electron poor) pyridines. Sharp, separate signals, as reported in reference 9+ESI, are observed for systems in 'slow' exchange on the NMR time scale.[9]

d.   General considerations regarding coalescence

The coalescence conditions of resonances v_A and v_B are dependent on a several factors (exchange rate at a given temperature, accessible temperature range of the solvent, signal separation of the exchanging resonance frequencies in Hz) and hardware (probe temperature window, spectrometer frequency) and therefore may or may not be observed.[5]

Examples for typical parameters of real-life measurements, with signal separation of exchanging peaks (Δv_{AB}), spectrometer frequencies and exchange rates ($k(T)$) are given below. The relationship between these parameters is represented by the equation $k(T) = \frac{\pi \Delta v_{AB}}{\sqrt{2}} \approx 2.22 \, \Delta v_{AB}$.[4]

In case coalescence between coupling constants happens, it can be approximated as $k(T) = \pi \frac{\sqrt{(v_1 - v_2)^2 + 6(J_{a1b1} * J_{a2b2})}}{\sqrt{2}}$,[6] where v_1 and v_2 are the resonance frequencies of the same proton in the two different states of ligand A, J_{a1b1} is the coupling constant observed for v_1, J_{a2b2} is the coupling constant observed for v_2.

A *para*-substituted pyridine has an AA'BB' (AA'XX') spin system. The discussion below focuses on the exchange process of H$_a$ of such a pyridine ligand.

As shown in Table S2, coalescence of H$_a$ at 300 MHz is seen k(T) = 50 Hz, at which rate the signals remain separate, even if broadened at 900 MHz. Thus, coalescence for the same exchange system can be seen only at higher temperature at higher magnetic field. As shown in Table S3, the chemical shift separation of the exchanging peaks also has a pronounced effect on the signal shape and point of coalescence, just as the signal linewidth (Table S4), which is dependent on shimming, for example (quality of NMR tube, particles, oxygen content of the sample, etc)

We wish to emphasize that observation of 'separate signals' does not necessarily mean lack of chemical exchange and the presence of a single species in solution. To evaluate the presence of possible exchange variable temperature experiments (influencing the exchange rate) and detection at different field strengths are recommended, in addition to EXSY (NOESY) experiments.

Table S2: Predicted NMR spectra using the model system shown in Figure S19 and Table S1. were simulated using the software gNMR (Version 5.0.6.0, P.H.M. Budzelaar, IvorySoft).
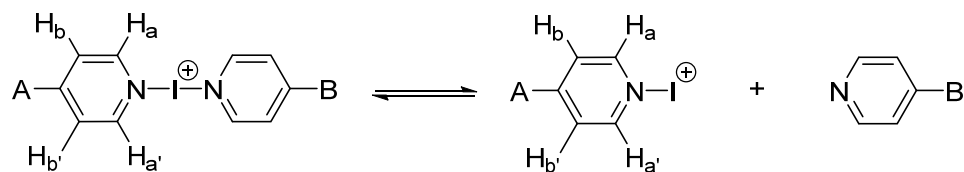

Figure S19: The system used for modelling the influence of dynamic exchange on a pyridine spin system.

The coalescence point depends on spectrometer frequency, and on the chemical shift separation of the exchanging peaks, thus δH_a in the [bis(pyridine)iodine(I)] complex and in the free ligand.
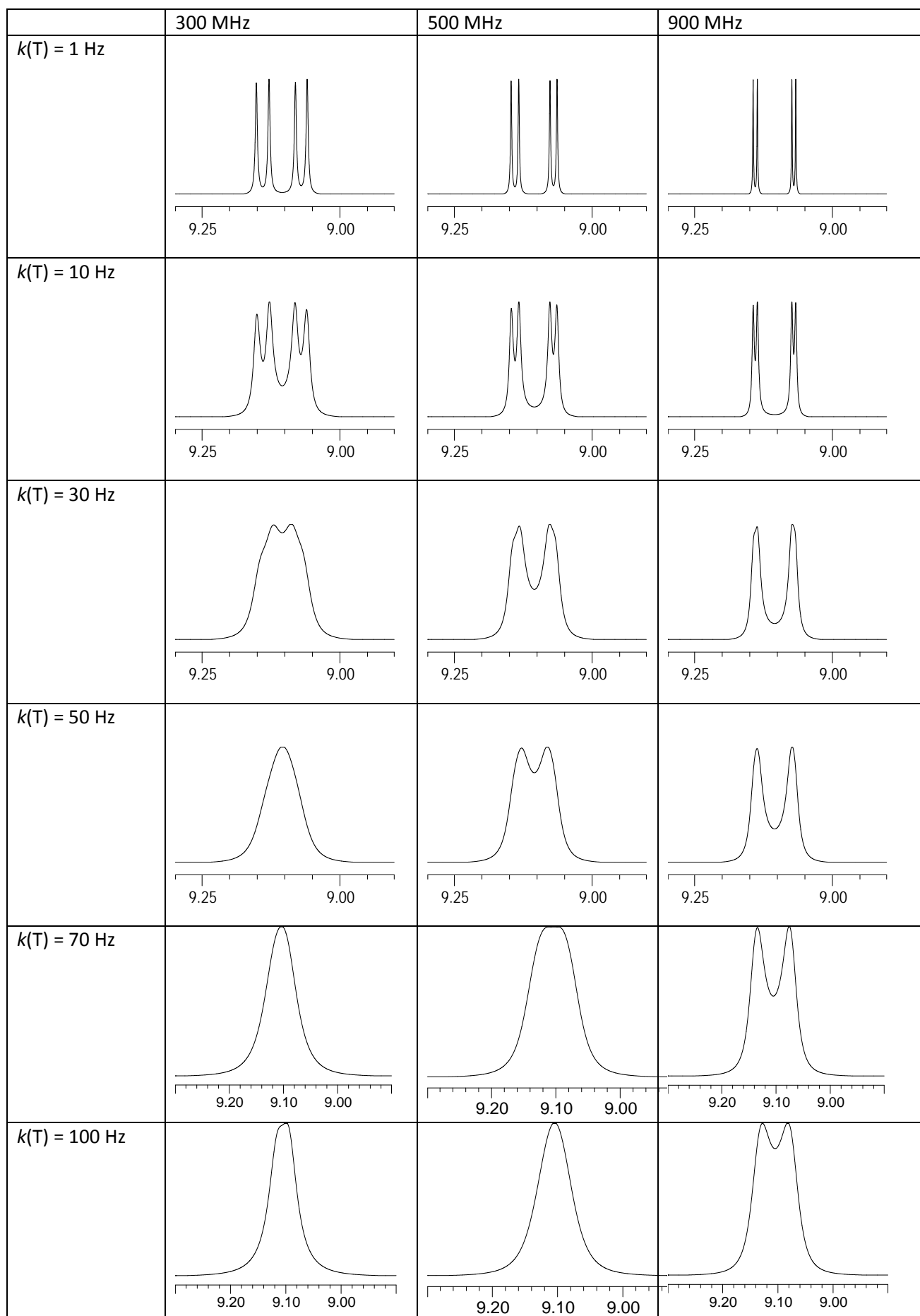
Table S1: Chemical shifts used in the simulations.

	Chemical shift δ [ppm] (J [Hz])			
Pyridine complex	H_a	$H_{a'}$	H_b	$H_{b'}$
A_1-I-B	9.07 (6.40)	9.07 (6.40)	7.88 (6.40)	7.88 (6.40)
A_2I	9.14 (6.90)	9.14 (6.90)	7.89 (6.90)	7.89 (6.90)

As shown in Table S2, coalescence of H_a at 300 MHz is seen k(T) = 50 Hz, at which rate the signals remain separate, even if broadened at 900 MHz. Thus, coalescence for the same exchange system can be seen only at higher temperature at higher magnetic field. As shown in Table S3, the chemical shift separation of the exchanging peaks also has a pronounced effect on the signal shape and point of coalescence, just as the signal linewidth (Table S4), which is dependent on shimming, for example (quality of NMR tube, particles, oxygen content of the sample, etc)

We wish to emphasize that observation of 'separate signals' does not necessarily mean lack of chemical exchange and the presence of a single species in solution. To evaluate the presence of possible exchange variable temperature experiments (influencing the exchange rate) and detection at different field strengths are recommended, in addition to EXSY (NOESY) experiments.

Table S2: Predicted NMR spectra using the model system shown in Figure S19 and Table S1.

	300 MHz	500 MHz	900 MHz
k(T) = 1 Hz			
k(T) = 10 Hz			
k(T) = 30 Hz			
k(T) = 50 Hz			
k(T) = 70 Hz			
k(T) = 100 Hz			

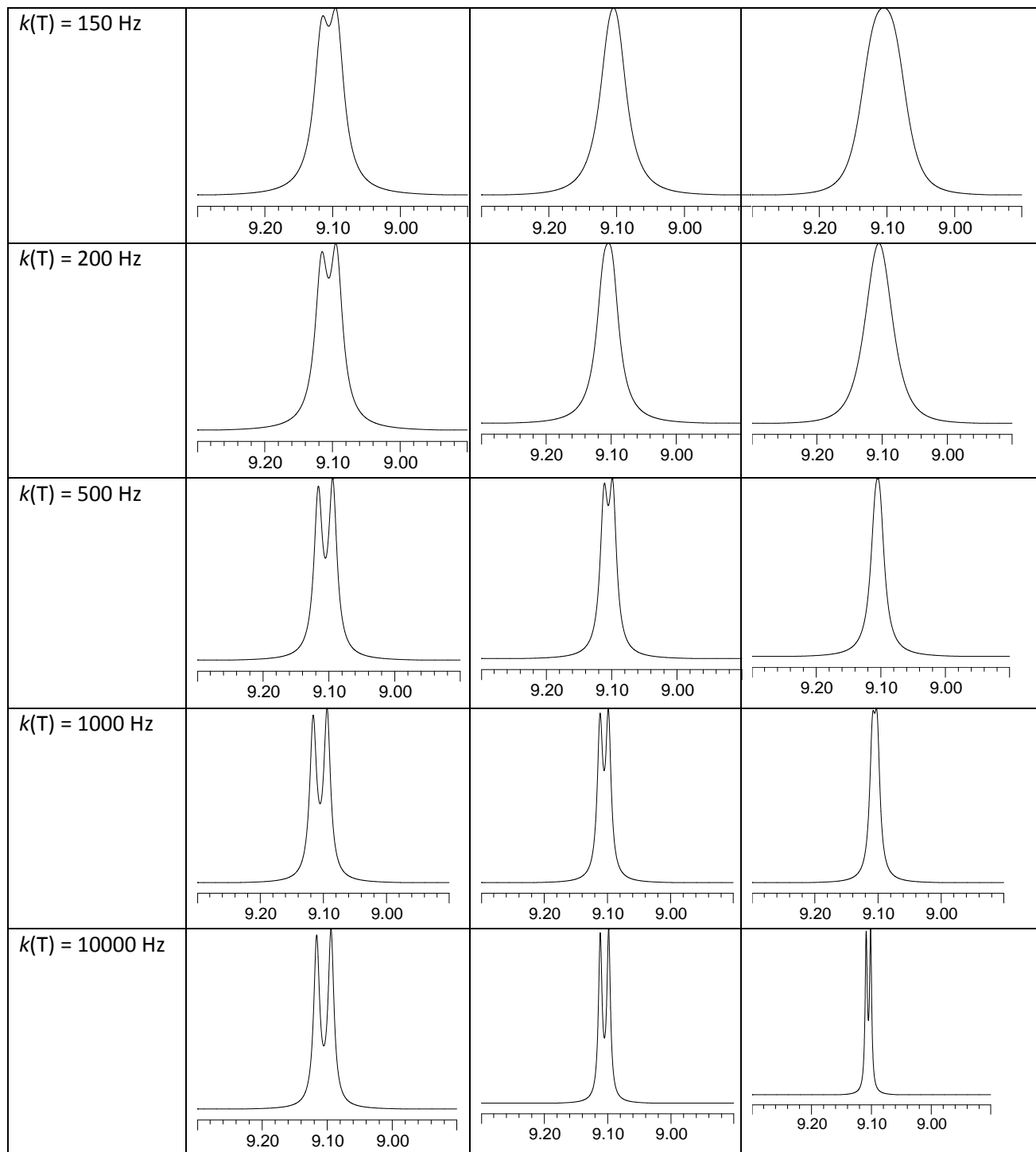| $k(T) = 150$ Hz			
	9.20 9.10 9.00	9.20 9.10 9.00	9.20 9.10 9.00
$k(T) = 200$ Hz			
	9.20 9.10 9.00	9.20 9.10 9.00	9.20 9.10 9.00
$k(T) = 500$ Hz			
	9.20 9.10 9.00	9.20 9.10 9.00	9.20 9.10 9.00
$k(T) = 1000$ Hz			
	9.20 9.10 9.00	9.20 9.10 9.00	9.20 9.10 9.00
$k(T) = 10000$ Hz			
	9.20 9.10 9.00	9.20 9.10 9.00	9.20 9.10 9.00

Table S3: Predicted NMR spectra using the model system shown in Figure S19 with a constant 100 Hz exchange rate and varying chemical shift differences ($\Delta\delta$) of H_α, upon keeping its chemical shift in A_1-I-B at 9.07 ppm, and altering Ha of A_2I (9.07, 9.14, 9.28, 9.35, 9.37, 9.77 ppm)

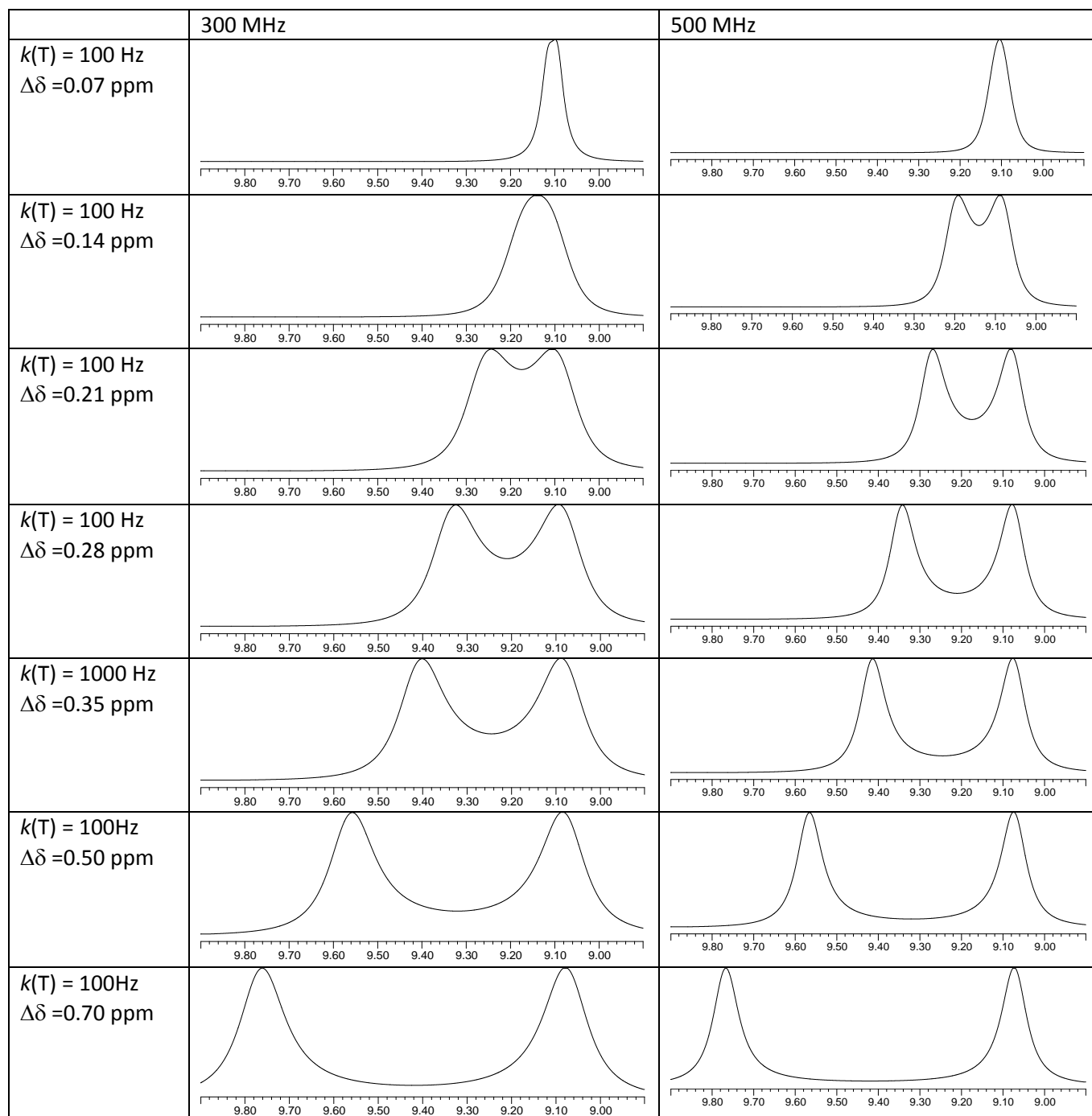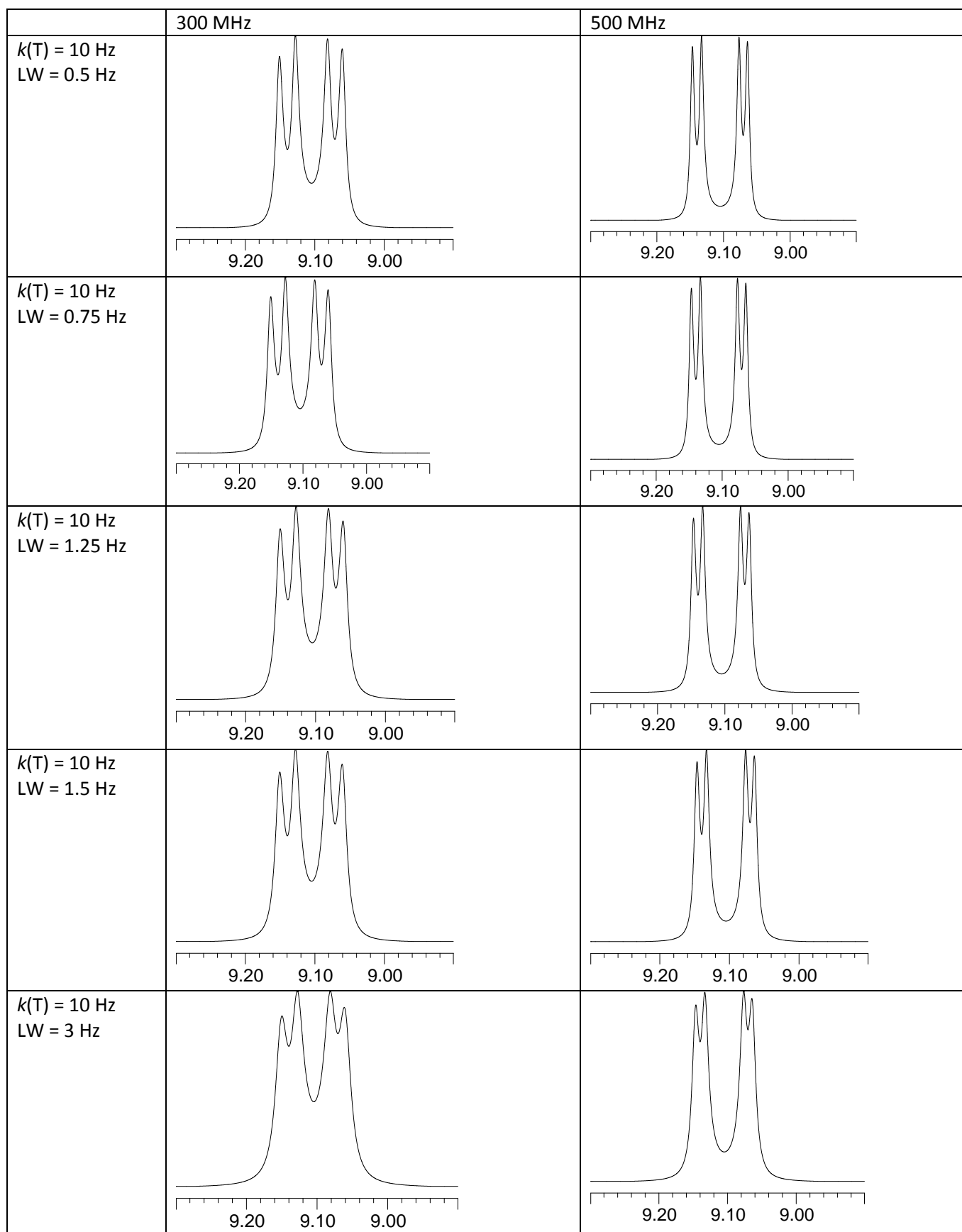|	300 MHz	500 MHz
k(T) = 100 Hz $\Delta\delta$ =0.07 ppm		
k(T) = 100 Hz $\Delta\delta$ =0.14 ppm		
k(T) = 100 Hz $\Delta\delta$ =0.21 ppm		
k(T) = 100 Hz $\Delta\delta$ =0.28 ppm		
k(T) = 1000 Hz $\Delta\delta$ =0.35 ppm		
k(T) = 100Hz $\Delta\delta$ =0.50 ppm		
k(T) = 100Hz $\Delta\delta$ =0.70 ppm		

Table S4: Predicted NMR spectra using the model system shown in Figure S19 with a 10 Hz exchange rate, chemical shifts as shown in Table S1. The linewidth (LW) of the signals, which may depend on shimming, is varied.

	300 MHz	500 MHz
k(T) = 10 Hz LW = 0.5 Hz		
k(T) = 10 Hz LW = 0.75 Hz		
k(T) = 10 Hz LW = 1.25 Hz		
k(T) = 10 Hz LW = 1.5 Hz		
k(T) = 10 Hz LW = 3 Hz		

3. Mixed [bis(pyridine)iodine(I)]⁺-type complexes

a. Mixture of [bis(2-fluoropyridine)iodine(I)]BF₄ ([(3)₂I]) with pyridine (1)

Mixing [bis(2-fluoropyridine)iodine(I)]BF₄ (10 mg, 0.024 mmol, 1.0 eq.) with pyridine (2.2 µL, 2.2 mg, 0.27 mmol, 1.12 eq.) in dry CD₃CN resulted in a clear colourless solution. The ^{1}H NMR spectrum of this mixture was measured and compared with the ^{1}H NMR spectra of the pure constituents. Very broad signals were observed with ^{1}H NMR.
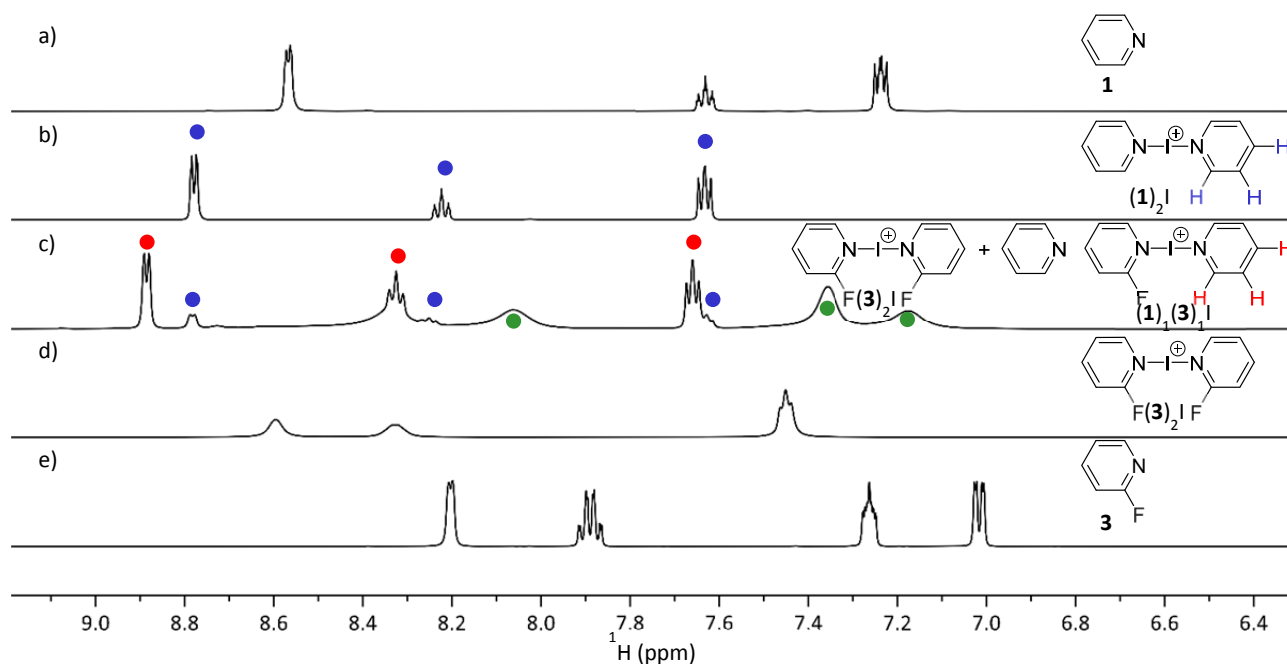

Figure S20: ^{1}H (500 MHz, CD₃CN, 298 K) of a) pyridine (1); b) [(1)₂I]; c) a 1.0:1.1 mixture of [(3)₂I] and 1; d) [(3)₂I]; e) and 2-fluoropyridine (3). Fast exchanging 2-fluoropyridine (3) (green dots).

b. Mixture of [bis(4-trifluoromethylpyridine)iodine(I)]BF$_4$ ([(4)$_2$I]) and pyridine (1)

Mixing a 0.6 mL solution of [bis(4-trifluoromethylpyridine)iodine(I)]BF$_4$ (7.6 mg, 0.015 mmol, 1.0 eq.) in dry CD$_2$Cl$_2$, tetraethylsilane (internal standard, 1.0 μL) and with pyridine (0.67, 1.33 and 2.70 equivalents , from a stock solution in CD$_2$Cl$_2$, 20 μL mL^{-1}, 0.25 mmol mL^{-1}, added, 20 μL, 40 μL, 100 μL) resulted in a clear and colourless solution. The ^{1}H and ^{15}N NMR spectra of this complex were compared with those of the pure compounds.
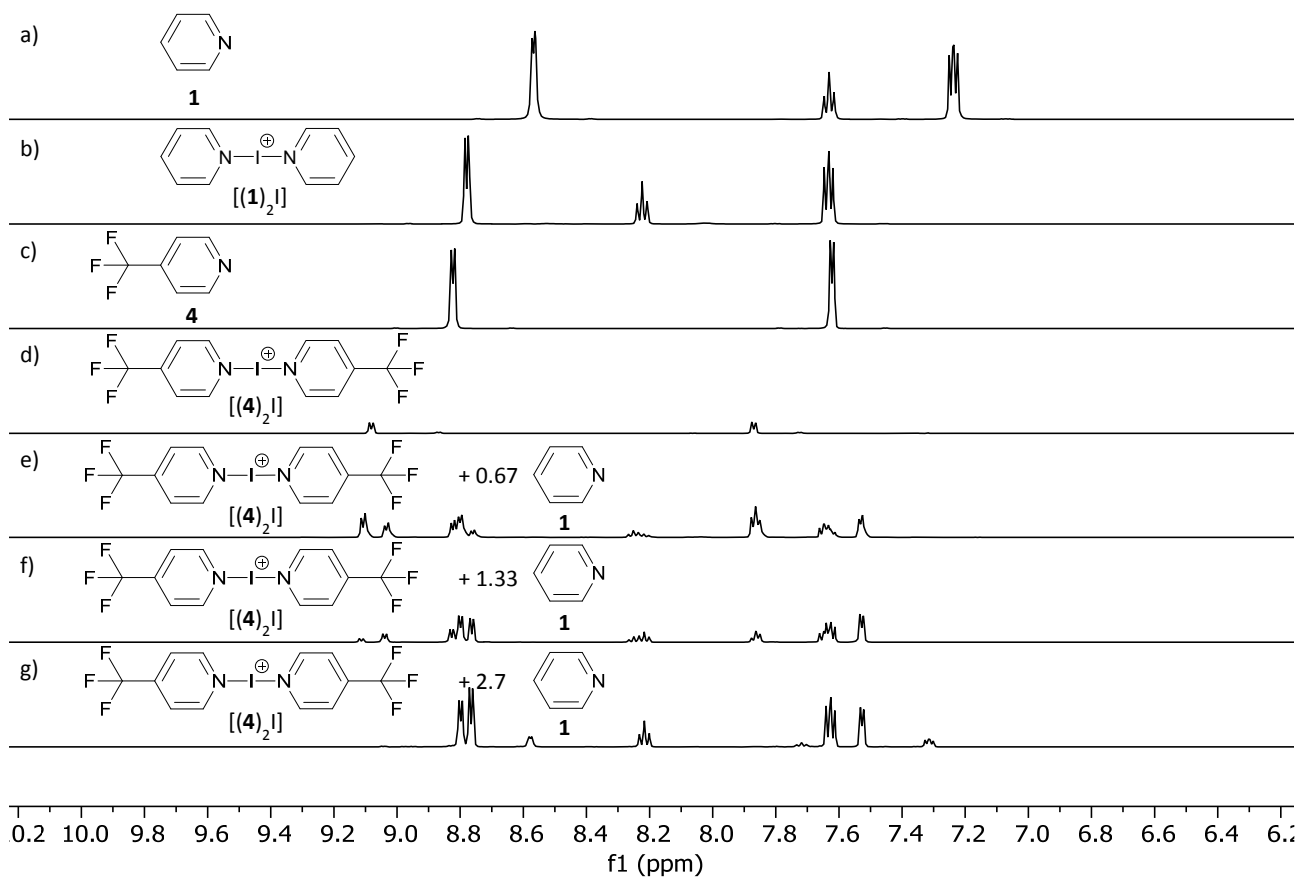

*Figure S21: ^{1}H (500 MHz,CD$_2$Cl$_2$, 298 K). a) Pyridine; (**1**); b) [Bis(pyridine)iodine(I)]BF$_4$ ([(**1**)$_2$I]); c) 4-Trifluoromethylpyridine (**4**); d) [Bis(4-trifluoromethylpyridine)iodine(I)]BF$_4$ ([(**4**)$_2$I]); e) Bis(4-trifluoromethylpyridine)iodine(I)]BF$_4$ ([(**4**)$_2$I]) + 0.67 eq. pyridine (**1**); f) 0.75:1.00 [Bis(4-trifluoromethylpyridine)iodine(I)]BF$_4$ ([(**4**)$_2$I]) and pyridine (**1**). g) [Bis(4-trifluoromethylpyridine)iodine(I)]BF$_4$ ([(**4**)$_2$I]) + 2.7 eq. pyridine (**1**).*
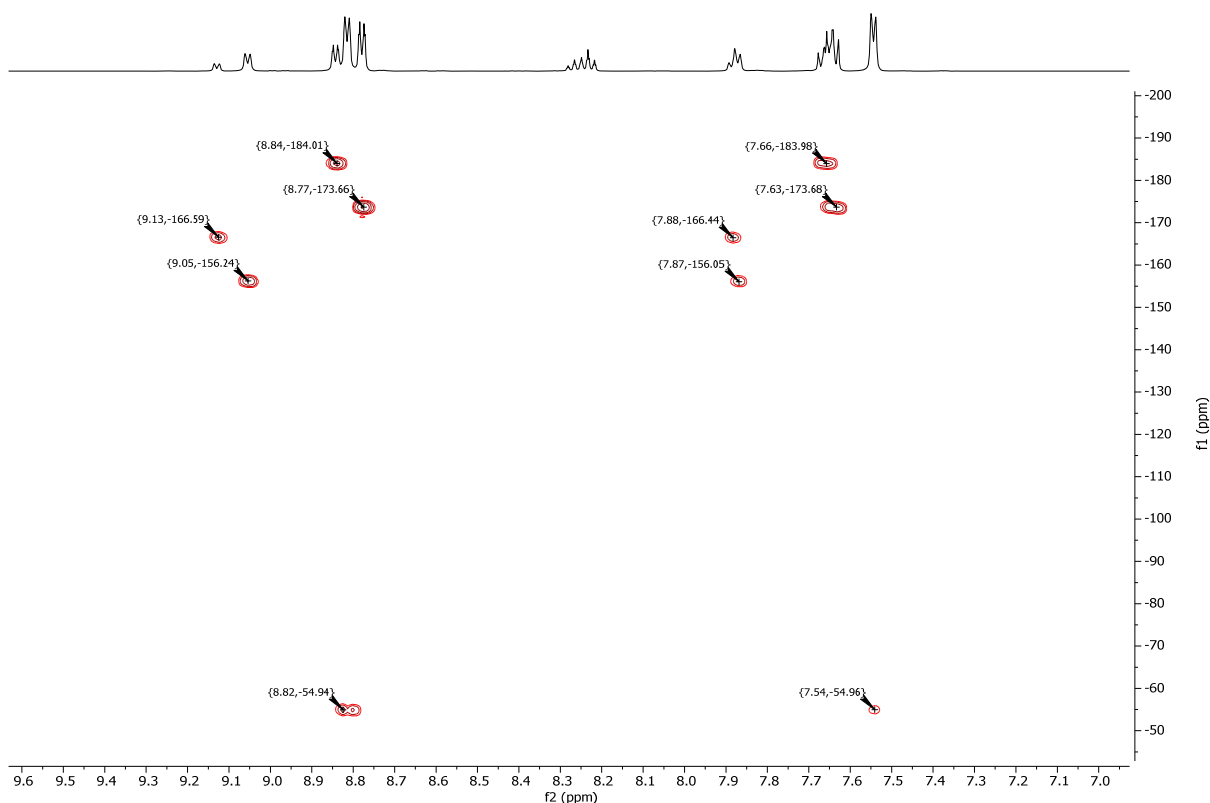
*Figure S22: $^1H^{15}N$ HMBC (51/500 MHz, CD_2Cl_2, 298 K) of 0.75 eq. [bis(4-trifluoromethylpyridine)iodine(I)]BF_4 ([(**4**)$_2$I]) + 1.00 eq. pyridine (**1**). [(**1**)$_2$I] (^{15}N (CD_2Cl_2, 298 K) = −174 ppm), [(**4**)$_2$I] (^{15}N (CD_2Cl_2, 298 K) = −166 ppm), **3** (^{15}N (CD_2Cl_2, 298 K) = −55 ppm).*

Adding sub-stoichiometric amounts of pyridine (**1**) to a CD_2Cl_2 solution of [bis(4-trifluoromethyl-pyridine)iodine(I)] BF_4 ([(**4**)$_2$I]) resulted in a mixture of the symmetric bis(pyridine)complexes [(**1**)$_2$I] and [(**4**)$_2$I] and ligand **4**, ^{15}N (CD_2Cl_2, 298 K) = −55 ppm), with a preference of releasing the less Lewis basic pyridine as a free species. In addition, a single additional mixed species, [(**1**)(**4**)I], is formed (^{15}N (CD_2Cl_2, 298 K) = −156, −184 ppm). The ^{15}N NMR spectroscopic investigation of the 1:1 mixture (Figure S21f) showed four ^{15}N resonances in the chemical shift range typical for iodine(I) complexes.[2,3,7,8] The resonances at −166 ppm and −174 ppm were assigned to [bis(4-trifluoromethylpyridine)iodine(I)]BF_4 [(**4**)$_2$I] and [bis(pyridine)iodine(I)] [(**1**)$_2$I] complexes. The resonances at −156 and −184 ppm belong to two different pyridine ligands, 4-trifluoromethylpyridine and pyridine, respectively, as part of the same complex, based on ^1H NMR integrals. This is a strong indication for the formation of an asymmetric [bis(pyridine)iodine(I)]-type complex, as proposed by Rissanen and coworkers in reference 3.[3] The ^{15}N NMR chemical shifts observed for this [(**1**)$_1$(**4**)$_1$I] complex shows stronger shielding of the pyridine nitrogen and less shielding of the 4-trifluoropyridine (**4**) nitrogen resonances as compared to the corresponding symmetric [bis(pyridine)iodine(I)]$^+$-type complexes. This observation suggests competitive binding situation, where strong binding of one ligand might weaken the binding of the second. Such a difference in the ^{15}N NMR chemical shifts in an asymmetric [bis(pyridine)iodinine(I)]$^+$-type complex has previously been reported in J. Am Chem. Soc. 2018, 140, 13503.

c. Variable temperature NMR study of a mixture of [bis(4-trifluoromethylpyridine)iodine(I)]BF$_4$ ([(4)$_2$I]) and pyridine (1)

Mixing a 0.6 mL solution of [bis(4-fluoropyridine)iodine]BF$_4$ (7.6 mg, 0.015 mmol, 0.75 eq.) in dry CD$_2$Cl$_2$ with tetraethylsilane (internal standard, 1.0 μL) and 1.0 equivalent of pyridine (stock solution in CD$_2$Cl$_2$, 20 μL mL^{-1}, 0.25 mmol mL^{-1}, added 40 μL) resulted in a clear and colourless solution. The ^{1}H NMR spectra of this mixture at different temperatures is reported (15 min equil. time, after adjusting the temperature).

The 0.75:1 mixture of [(4)$_2$I] and **1** was stable in the investigated temperature range of 278 K–308 K. With increasing temperature, increasing line broadening was observed. The signals of every complex experienced line broadening, with that of [(1)$_1$(4)$_1$I] having been most pronounced. The ^{1}H NMR signals of the observed species were integrated, and their concentrations estimated based on the integral of the internal SiEt$_4$ standard that is not involved in any exchange process. The spectra shown in Figure S24 indicated no detectable temperature dependence of the composition of the mixture within the 278 K–308 K temperature interval.
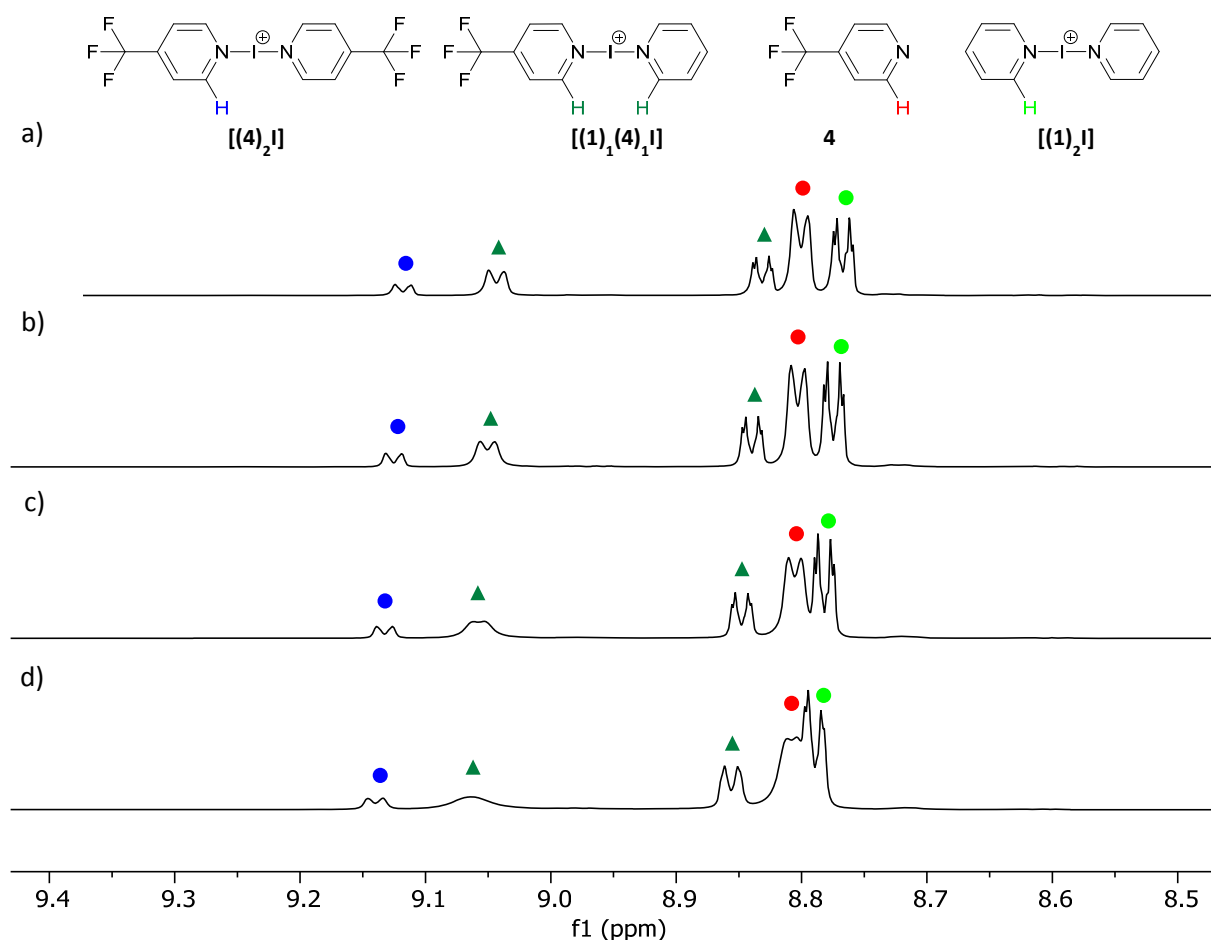

Figure S23: ^{1}H (500 MHz, CD$_2$Cl$_2$) of a 0.75:1 mixture of [bis(4-trifluoromethylpyridine)iodine(I)]BF$_4$ ([(4)$_2$I]BF$_4$) and pyridine (**1**) at the temperatures a) 278.2 K; b) 288.2 K; c) 298.2 K; d) 308.2 K. Blue dot (●): [(4)$_2$I]; dark green triangle (▲): [(1)$_1$(4)$_1$I]; light green circle (●): [(1)$_2$I]; red dot (●): free **4**.

a)

b)

c)

d)

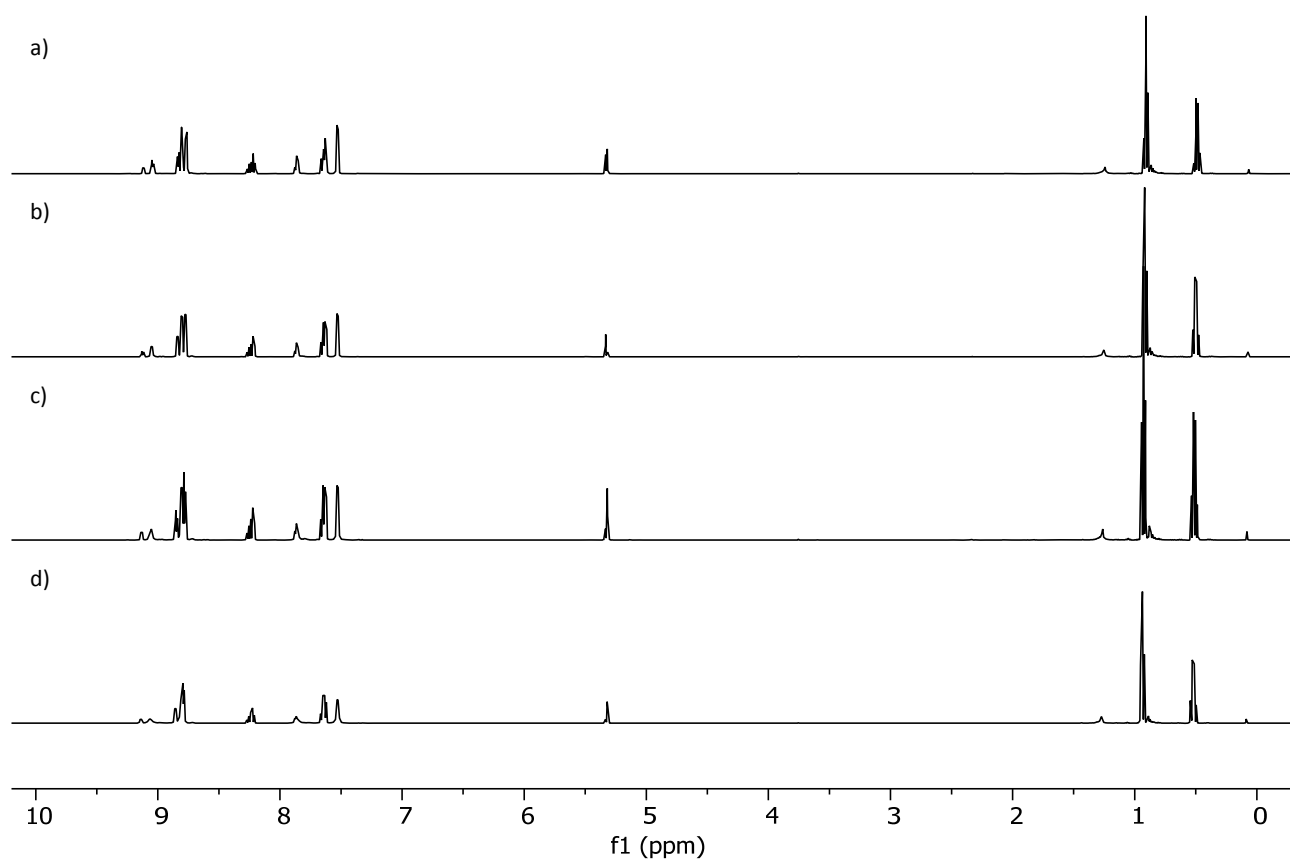|										
10	9	8	7	6	5	4	3	2	1	0

f1 (ppm)

Figure S24: ^{1}H (500 MHz, CD$_2$Cl$_2$) of a 0.75:1 mixture of [(4)$_2$I] and 1 at the temperatures a) 278 K; b) 288 K; c) 298 K; and d) 308 K.
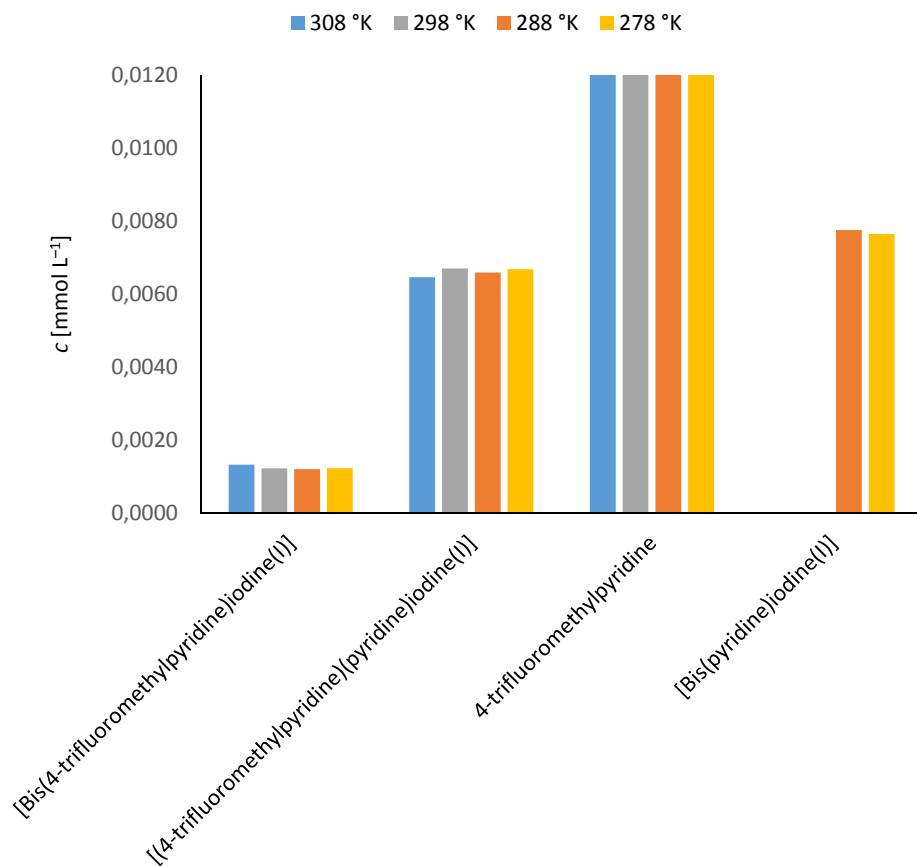
*Figure S25: Temperature dependent integral ratio of compounds present after mixing 0.75 eq. [bis(4-trifluoromethylpyridine)iodine(I)]BF$_4$ with 1.0 eq. pyridine in CD$_2$Cl$_2$. The ^{1}H NMR integrals are given relative to the internal SiEt$_4$ standard. At 308 and 298 K no signal suitable to integrate the [bis(pyridine)iodine(I)] complex ([(**1**)$_2$I]) was observed due to signal overlaps.*

d.   The influence of temperature and dilution on [bis(4-trifluoromethylpyridine)iodine(I)]BF$_4$ ([(4)$_2$I]) in the presence of [bis(pyridine)iodine(I)]BF$_4$ ([(1)$_2$I])

Mixing a 0.5 mL solution of [bis(4-fluoropyridine)iodine(I)]BF$_4$ (5 mg, 0.098 mmol, 1.0 eq.) in dry CD$_2$Cl$_2$, with a 0.5 mL solution of [bis(pyridine)iodine(I)]BF$_4$ (3.7 mg, 0.099 mmol, 1.0 eq.) in dry CD$_2$Cl$_2$ resulted in a colourless solution. The resulting mixture was left for 1 h to equilibrate, and subsequently NMR spectra were acquired. A 0.050 mL portion of this sample was diluted with 0.950 mL CD$_2$Cl$_2$. The concentration of the observed species was calculated based on the relative signal intensities, and the known total content of individual pyridine ligands using the equation:

$$n(py) + n(pCF_3py) = \sum_{n=1}^{NMR\ signal\ (m)} \left[\frac{I_n}{I_{total}} \middle/ \sum_{n=1}^{NMR\ signal\ (m)} \frac{I_n}{I_{total}} \right] * \left[\frac{x_n * f_{normalization\ factor}}{z_n} \right]$$

with, z_n being the signal corresponding proton count of the species/signal n, x_n the number of the form of ligands corresponding to species n, I_n the intensity of the signal corresponding to species n, I_{total} the total intensity of all signals that are taken into account.

The 1:1 mixture of [bis(4-trifluoromethylpyridine)iodine(I)]BF$_4$ and [bis(pyridine)iodine(I)]BF$_4$ forms an equilibrium consisting of five different species (Table S5), as indicated by ^{1}H and ^{15}N NMR.
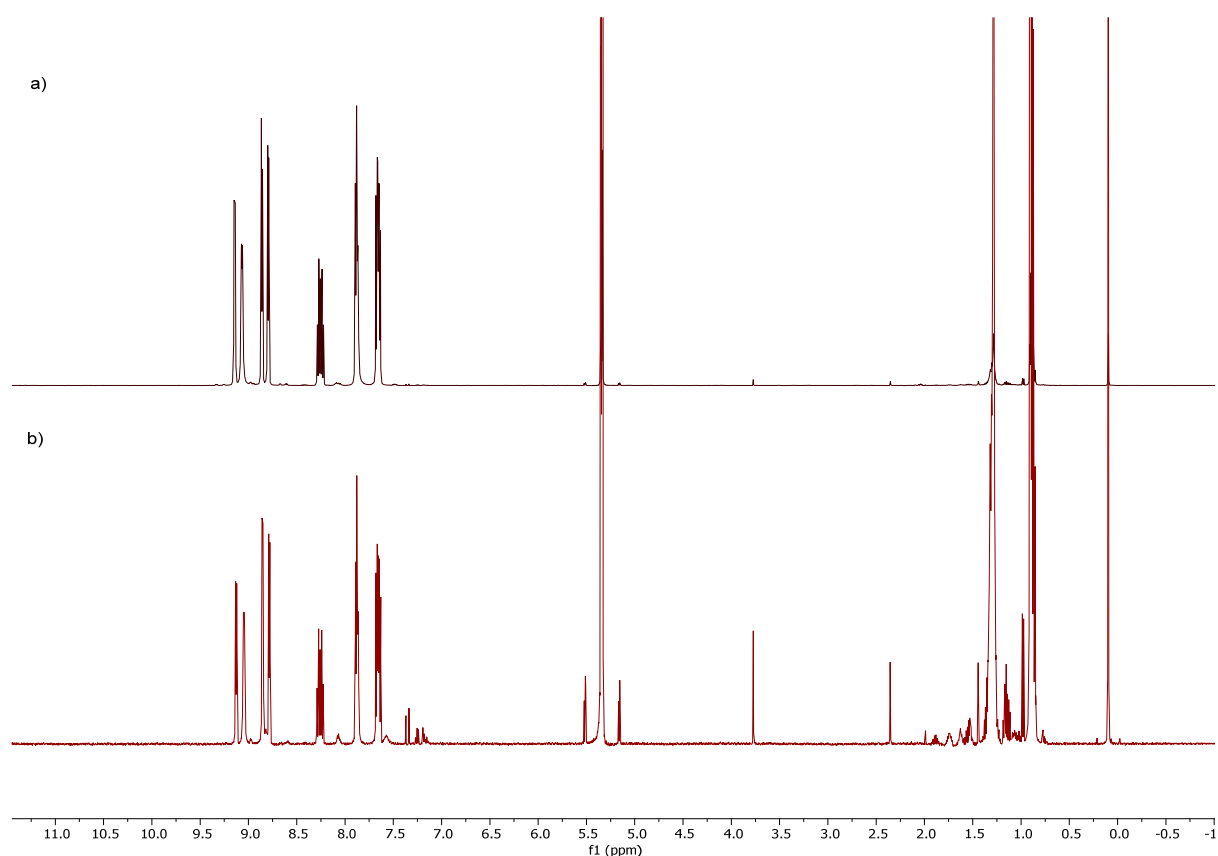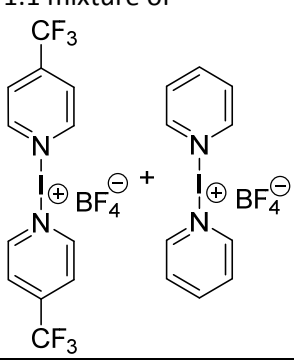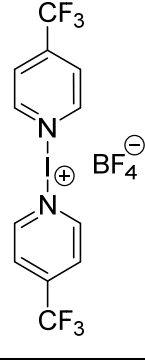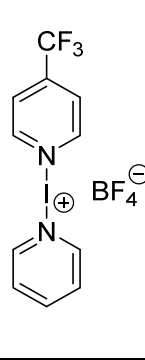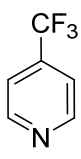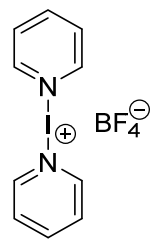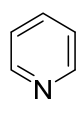

Figure S26: ^{1}H NMR spectrum of a solution of 0.010 M [bis(4-trifluoromethylpyridine)iodine(I)]BF$_4$ ([(4)$_2$I]BF$_4$) and 0.010 M [bis(pyridine)iodine(I)]BF$_4$ ([(1)$_2$I]BF$_4$) (top,) and 1:19 dilution of this mixture scaled by factor 20 (bottom).

Table S5: The molar ratio of the various species of [bis(pyridine)iodine(I)]⁺-type complexes and free ligands in CD₂Cl₂ at a total iodine(I) concentration of 0.020 M and 0.0010 M.

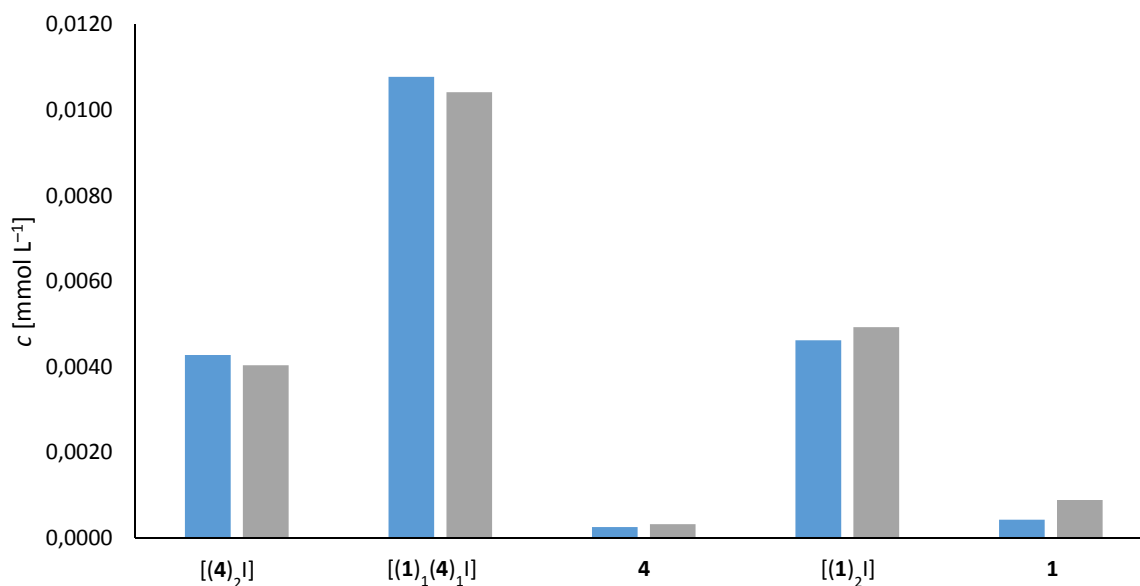| initial mixture	resulting concentrations in solution				
1:1 mixture of					
total iodine(I) concentration	c [mmol L⁻¹]	c [mmol L⁻¹]	c [mmol L⁻¹]	c [mmol L⁻¹]	c [mmol L⁻¹]
0.020 M solution	4.3	10.8	0.3	4.6	0.4
0.0010 M solution	0.20	0.52	0.02	0.25	0.04
0.0010 M solution × 20	4.0	10.4	0.3	4.9	0.9

Figure S27: The molar ratio of the various species of [bis(pyridine)iodine(I)] complexes in CD₂Cl₂ at a total iodine(I) concentration of 0.020 M (blue) and 0.0010 M (grey).
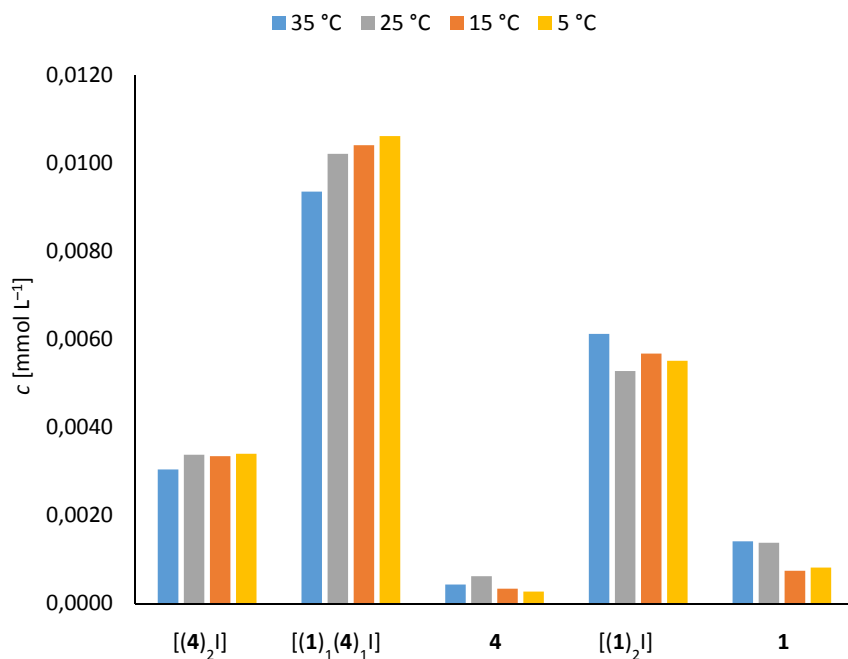
Figure S28: The molar ratio of various species of in a 1:1 mixture of [bis(pyridine)iodine(I)] complexes in CD$_2$Cl$_2$ at different temperatures, and at the total iodine(I) concentration of 0.020 M.

As indicated by Figures S21-S28, [bis(pyridine)iodine(I)] complexes undergo ligand exchange reactions. The equilibrium is insensitive (<10 rel%) to mild temperature (5–35°C) and concentration changes.

e. The influence of the molar ratio of [bis(4-trifluoromethylpyridine)iodine(I)]BF$_4$ ([(**4**)$_2$I]) and [bis(pyridine)iodine(I)]BF$_4$ ([(**1**)$_2$I]) on their exchange.

Stock solutions of [bis(4-fluoropyridine)iodine(I)]BF$_4$ ([(**4**)$_2$I]) (25.1 mg, 0.0492 mmol) and [bis(pyridine)iodine(I)]BF$_4$ ([(**1**)$_2$I]) (18.2 mg, 0.0487 mmol) in dry CD$_2$Cl$_2$ (2.50 mL each) was prepared. Five solutions with different ratios of stock solutions (0.90:0.10, 0.70:0.30, 0.30:0.30, 0.30:0.70, 0.10:0.90 mL) were prepared, and studied by NMR. The ^{1}H NMR signals of the observed species were integrated, and their molar ratios were calculated based on the applied total concentrations of the pyridines using the formula:

$$Share\ of\ compound\ n\ = \frac{I_n/z_n}{I_1/z_1 + I_2/z_2 + I_3/z_3}$$

with I_n being the intensity of a signal of compound n and z_n the number of equivalent protons that belong to signal I_n. We observed a statistical distribution of the pyridines in their iodine(I) complexes.
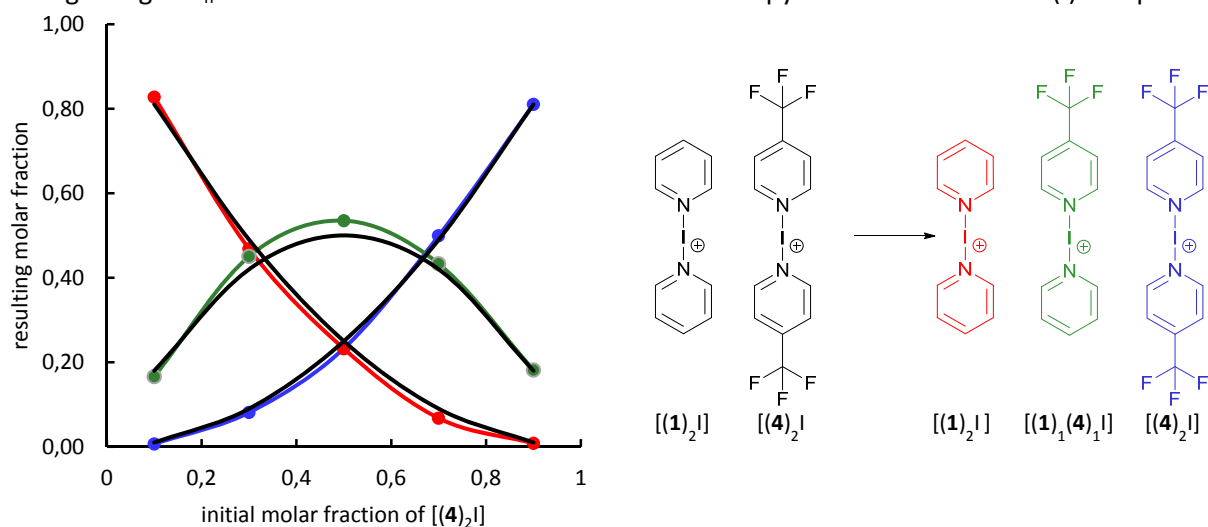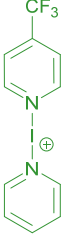

Figure S29: Mixtures of symmetric and asymmetric [bis(pyridine)iodine(I)] complexes based on an initial share of [(**4**)$_2$I] in a mixture with [(**1**)$_2$I], based on ^{1}H NMR integration in CD$_2$Cl$_2$ at 0.050 M total iodine(I) concentration. Red line [(**1**)$_2$I] ; green line [(**1**)(**4**)I]; blue line [(**4**)$_2$I]; black line: simulated expected contribution based on a purely statistical contribution of the ligands.

f. A mixture of [bis(4-trifluoromethylpyridine)iodine(I)]BF$_4$ ([(**4**)$_2$I]) and [bis(pyridine)iodine(I)]BF$_4$ ([(**1**)$_2$I]): the effect of excess 4-trifluoromethylpyridine (4)

Stock solutions of [bis(4-trifluoropyridine)iodine(I)] BF$_4$ ([(**4**)$_2$I]) (25.1 mg, 0.0492 mmol) and [bis(pyridine)iodine(I)]BF$_4$ ([(**1**)$_2$I]) (18.2 mg, 0.0487 mmol) in dry CD$_2$Cl$_2$ (2.50 mL each) have been prepared. Various ratios of stock solutions of the two components (0.30:0.30 mL) and 4-trifluoromethylpyridine (1200 μL, 10.4 μmol, 0.88 eq.) were mixed and studied by NMR.

*Table S6: The molar ratios of iodine(I) complexes observed in solution, following addition of 0.88 eq. of **4** to a 1:1 mixture of [(**4**)$_2$I]BF$_4$ and [(**1**)$_2$I]BF$_4$ in CD$_2$Cl$_2$ at r.t..*

	4	[(**1**)$_2$I]	[(**1**)$_1$(**4**)$_1$I]	[(**4**)$_2$I]
without		0.23	0.54	0.23
with		0.21	0.53	0.26

g. The MS(ESI) study of a mixture of [bis(4-trifluoromethylpyridine)iodine(I)]BF$_4$ ([(**4**)$_2$I]) and [bis(pyridine)iodine(I)]BF$_4$ ([(**1**)$_2$I]) and 4-trifluoromethylpyridine (**4**)

Mixing a 0.1 mL solution of [bis(4-fluoropyridine)iodine(I)]BF$_4$ ([(**4**)$_2$I]) (10 mg, 0.020 mmol, 1.0 eq.) in dry CH$_3$CN and 0.1 mL solution of [bis(pyridine)iodine(I)]BF$_4$ ([(**1**)$_2$I]) (7.33 mg, 0.020 mmol, 1.0 eq.) in dry CH$_3$CN, resulted in a clear and colourless solution. The resulting mixture was studied with MS(ESI). Mild ionisation conditions were used to observe all species present in solution.
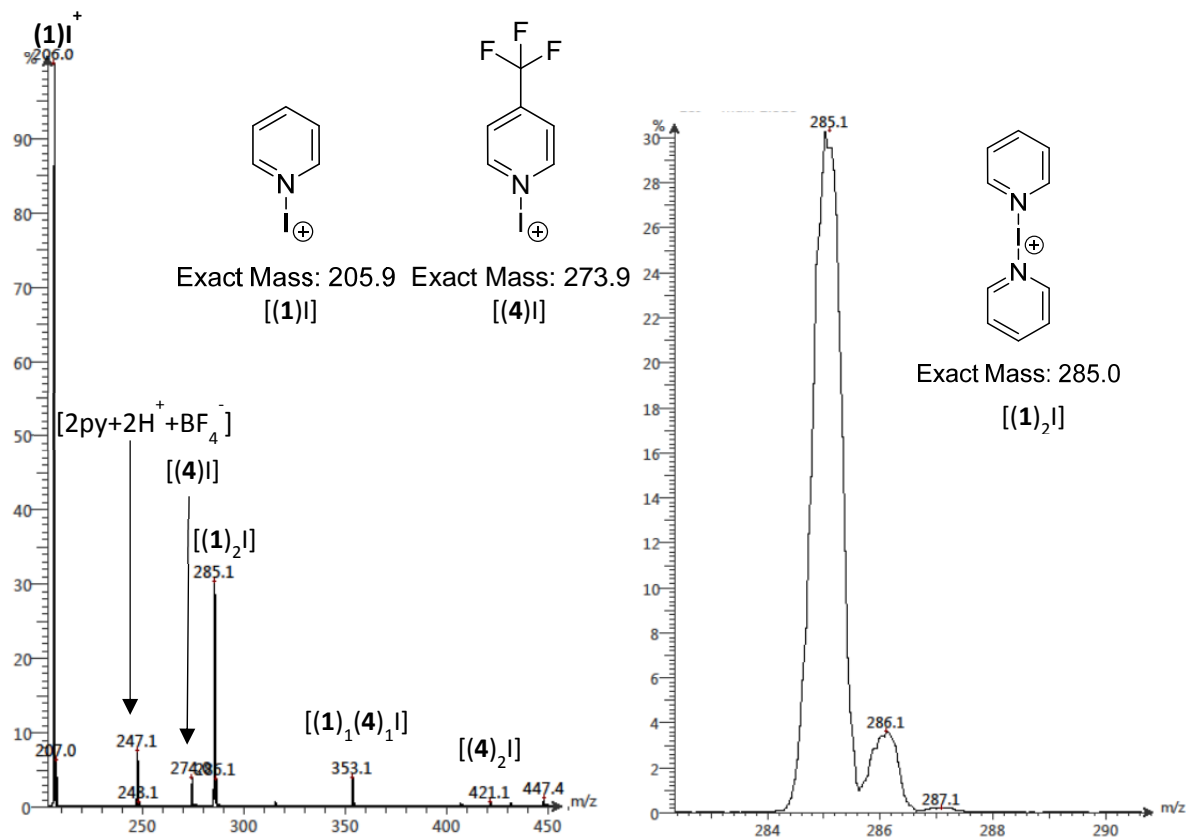

Figure 30: ESI MS (positive ion detection mode) histogram of a 1:1 mixture of [(**1**)$_2$I] and [(**4**)$_2$I]. MS(ESI) spectra showing all observed signals is given on the left, whereas a selected region showing the signal of [(**1**)$_2$I] on the right.
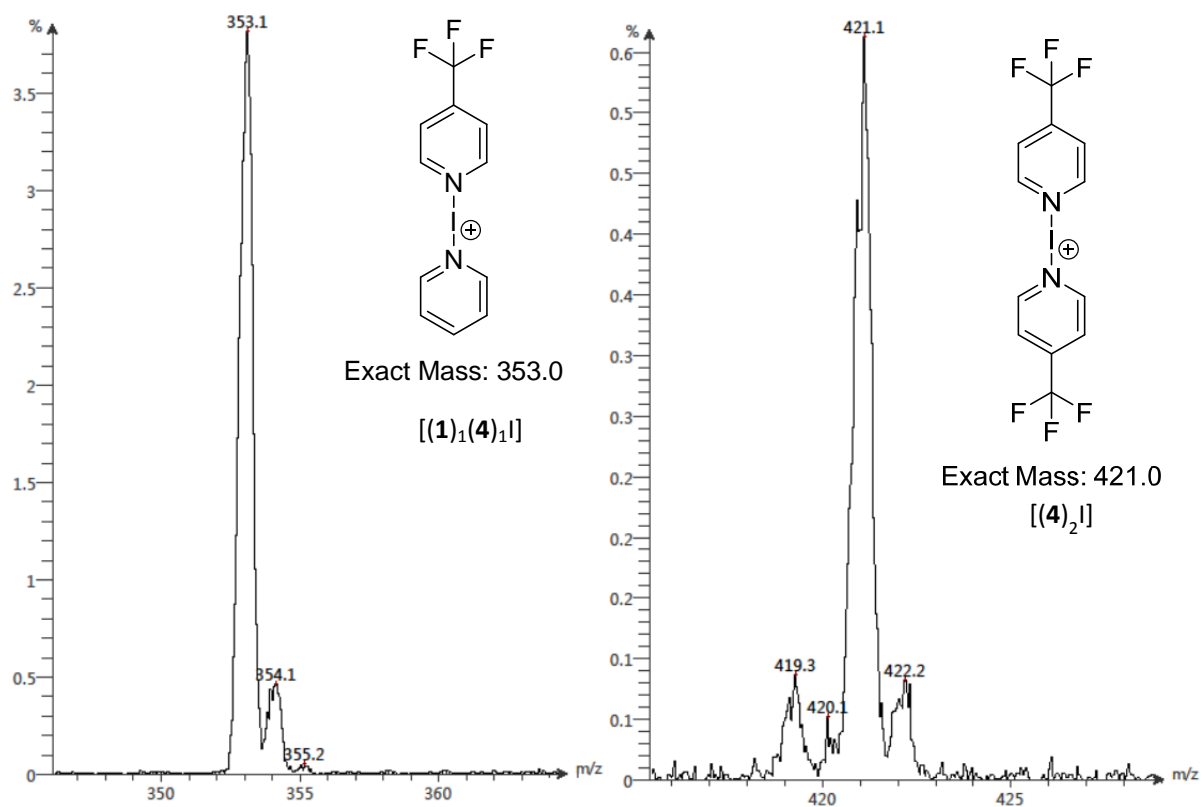
*Figure S31: MS(ESI) (positive ion detection mode) spectra of a 1:1 mixture of [(**1**)₂I] and [(**4**)₂I]. The MS(ESI) histogram showing the selected region of the full histogram (Figure 307) with the signal of [(**1**)₁(**4**)₁I] to the left, and [(**4**)₂I] to the right.*

h.   The influence of addition of 4-trifluoromethylpyridine (4) to a mixture of [bis(4-trifluoromethylpyridine)iodine(I)]BF$_4$ ([(4)$_2$I]BF$_4$) and [bis(pyridine)iodine(I)]BF$_4$ ([(1)$_2$I]BF$_4$)

Mixing a 0.6 mL solution of [bis(4-fluoropyridine)iodine(I)]BF$_4$ ([(4)$_2$I]BF$_4$) (10 mg, 0.020 mmol, 1.0 eq.) in dry CD$_2$Cl$_2$, tetraethylsilane (internal standard, 1.0 µL) and 1.0 equivalent of pyridine (1) (stock solution in CD$_2$Cl$_2$, 20 µL mL^{-1}, 0.25 mmol mL^{-1}, added 40 µL) resulted in a clear and colourless solution. The mixture was measured at different temperatures, with 15 min equilibration delays. Subsequently 1.0 eq of 4-fluoropyridine (4) was added.

The ^{1}H NMR signals of the observed species were integrated, and their concentrations calculated based on the integral of the internal reference SiEt$_4$. No influence of the addition of an additional equivalent of 4-trifluoromethylpyridine (4) on the observed equilibrium was observed.

The absence of a detectable effect on the equilibrium of [bis(pyridine)iodine(I)]$^+$-type species suggests a dominant enthalpic driving force in the iodine(I) complex formation. On the other hand the statistical distribution observed for mixtures of already formed iodine(I) complexes is caused by a potentially dominant entropic contribution. The distribution appears independent of the concentration of the weaker ligand. The [bis(4-fluoropyridine)-iodine(I)]BF$_4$ complex remains observable.
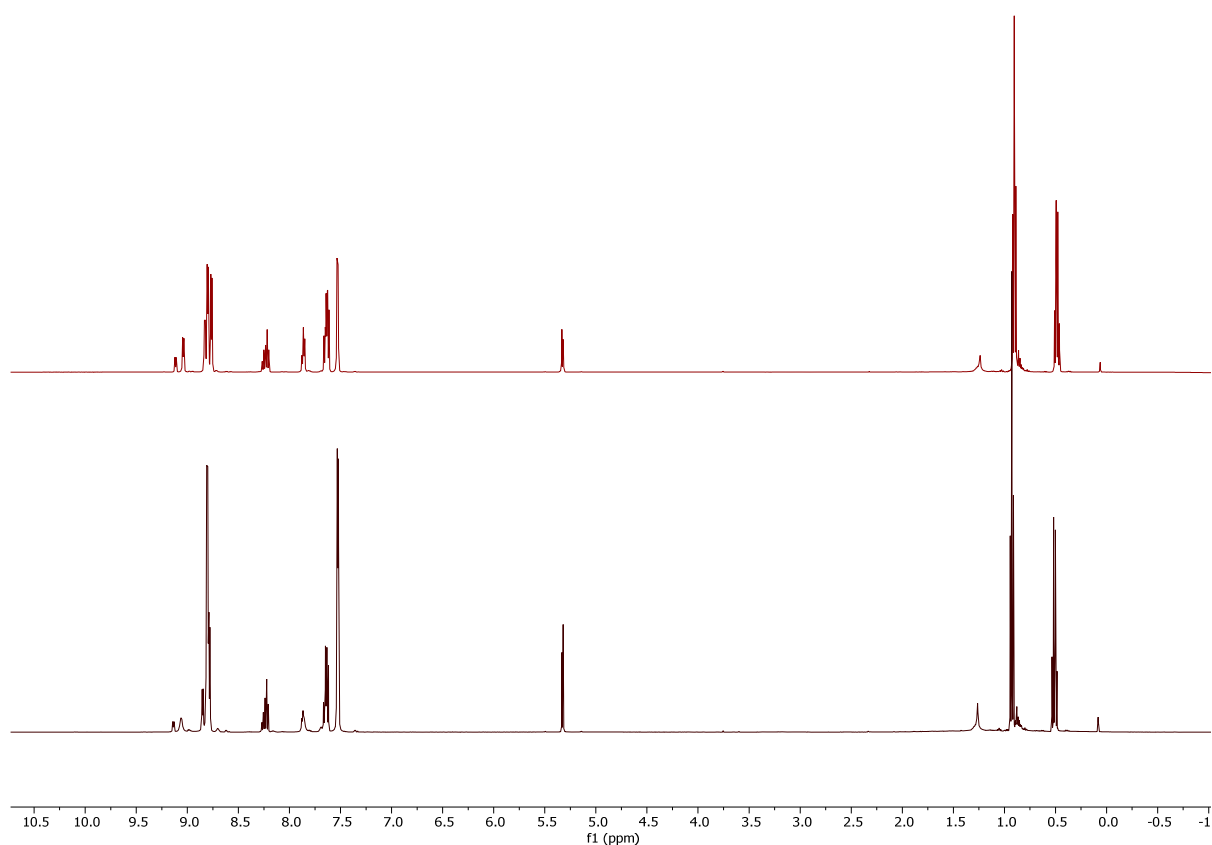

Figure S32: The ^{1}H NMR spectrum of a mixture of [bis(4-trifluoromethylpyridine)iodine(I)]BF$_4$ ([(4)$_2$I]BF$_4$) and [bis(pyridine)iodine(I)]BF$_4$, ([(1)$_2$I]BF$_4$)before (lower) and after the addition of 4-trifluoromethylpyridine (4) (upper).
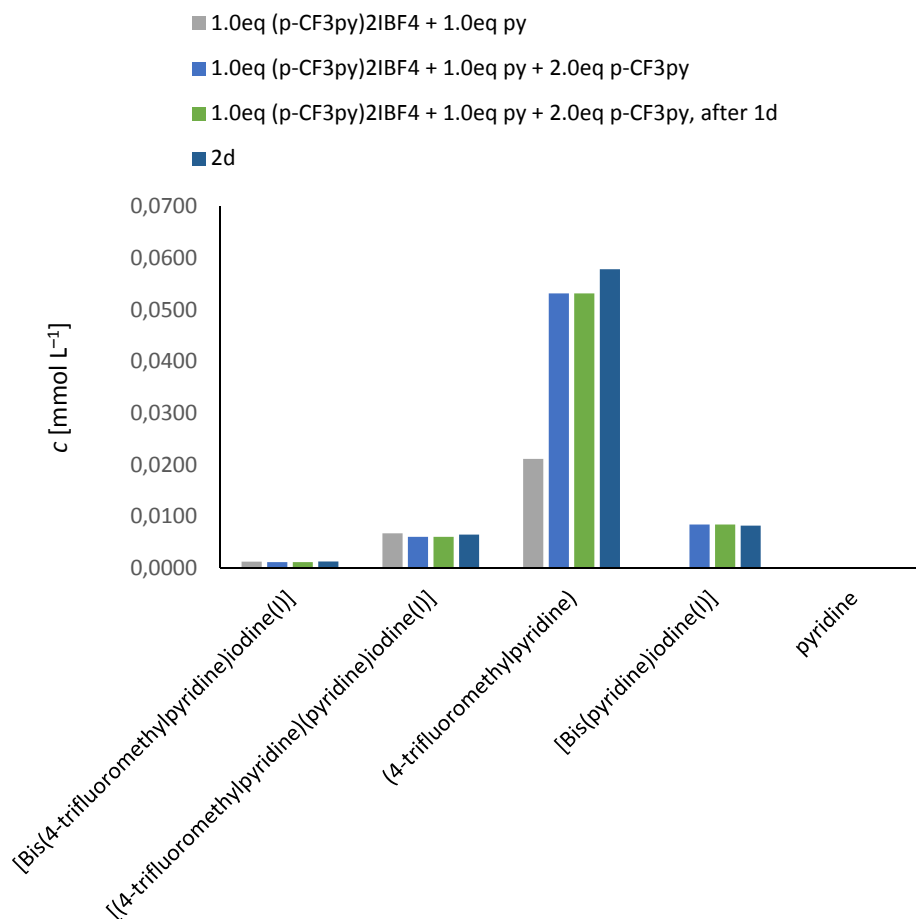
*Figure S33: The concentrations of various species observable in a mixture of [bis(4-trifluoromethyl-pyridine)iodine(I)]BF$_4$ ([(**4**)$_2$I]BF$_4$)and [bis(pyridine)iodine(I)]BF$_4$ ([(**1**)$_2$I]BF$_4$), upon addition of 4-trifluoromethylpyridine (**4**), and upon letting the sample stand.*

i. A mixture of [bis(4-ethylpyridine)iodine(I)]BF$_4$ ([(**5**)$_2$I]) and [bis(pyridine)iodine(I)]BF$_4$ ([(**1**)$_2$I])

[Bis(4-ethylpyridine)iodine(I)]BF$_4$ (21.4 mg, 0.050 mmol, 1.00 eq.) and [bis(pyridine)iodine(I)]BF$_4$ (18.4 mg, 0.049 mmol, 0.99 eq.) were dissolved in dry CD$_2$Cl$_2$ (1 mL) and the mixture was studied by NMR. The 1:1 mixture of [(**5**)$_2$I]BF$_4$ and [(**1**)$_2$I]BF$_4$ formed a stable mixture at room temperature.

In ^{1}H NMR and ^{13}C NMR, the number of peaks observed for each pyridine ligand indicates the formation of mixed species (Figure S34 and Figure S36). The signals are overlapping (Figure S35), but from the enlarged spectral window (Figure S34), it is clear that the observed signals match a 0.5:1:0.5 mixture of [(**1**)$_2$I]:[(**1**)$_1$(**5**)$_1$I]:[(**5**)$_2$I], with a signal ratio of 1:1:1. In the ^{1}H^{15}N HMBC spectrum (Figure S37), the shifts of [(**1**)$_2$I] ($\delta = -174$) and [(**5**)$_2$I] ($\delta = -181$) as well as the slightly shifted signals of a new species with pyridine-ligand ($\delta = -170$) and 4-ethylpyridine-ligand ($\delta = -184$) resonances are observed. The deshielding and shielding effect observed for the pyridine-type ligands in [(**1**)$_1$(**5**)$_1$I] are in line with that observed for other asymmetric, substituted bis(pyridine)-type iodine(I) complexes.[9] In comparison to its symmetric [bis(pyridine)iodine(I)]$^+$-type complex, the more basic pyridine is deshielded if the *trans*-ligand is a weaker pyridine base, while for the weaker pyridine ligand the opposite is observed.
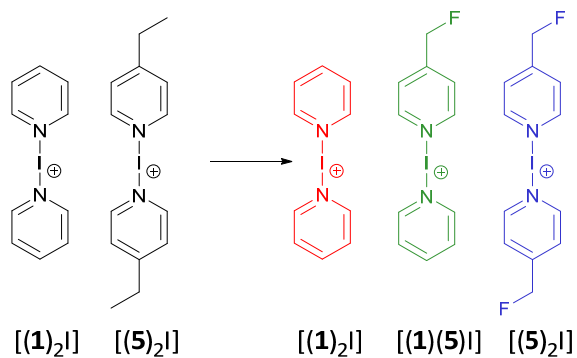
Figure S34: Observed reaction when dissolving a 1:1 mixture of [(**1**)₂I] and [(**5**)₂I] in CD₂Cl₂.
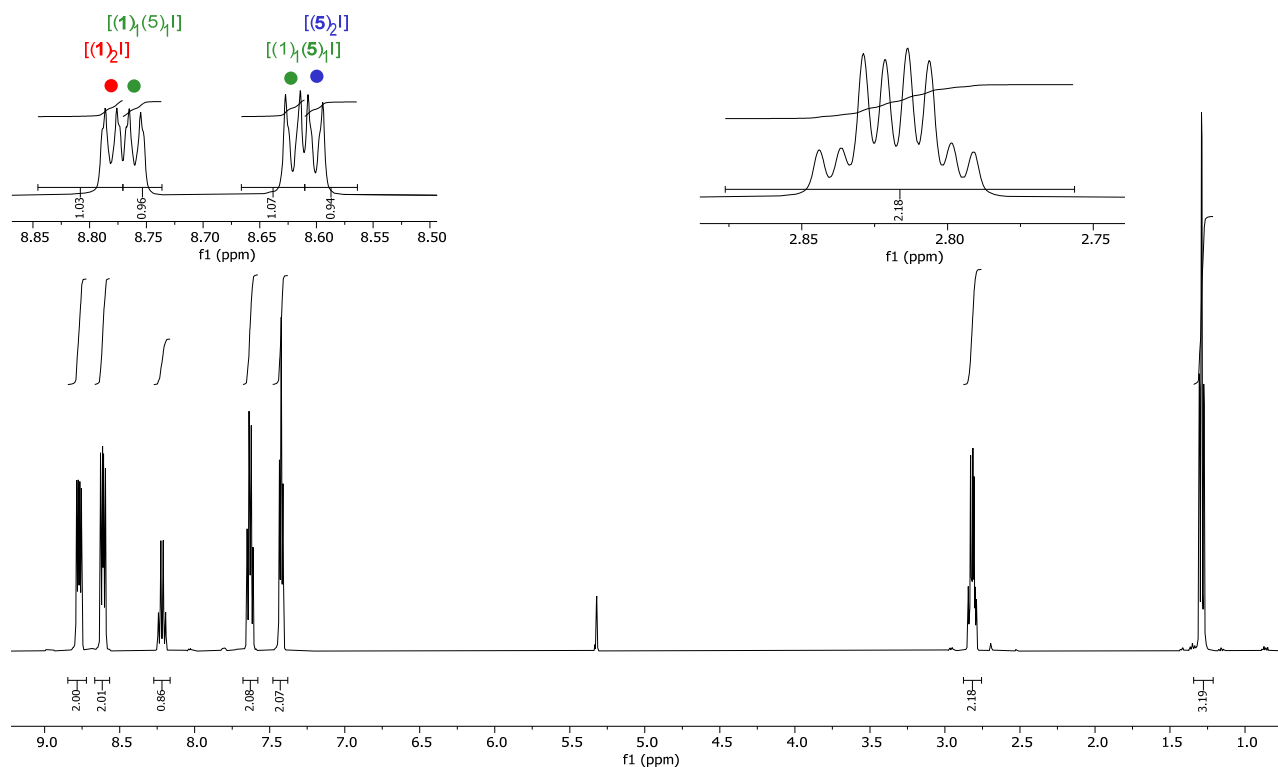

Figure S35: ¹H (400 MHz, CD₂Cl₂, 298 K) of a 1:1 mixture of [bis(4-(ethyl)pyridine)iodine(I)]BF₄ ([(**5**)₂I]) and [bis(pyridine)iodine(I)]BF₄ ([(**1**)₂I]). Selected regions are enlarged to demonstrate the doubling of the pyridine NMR signals.
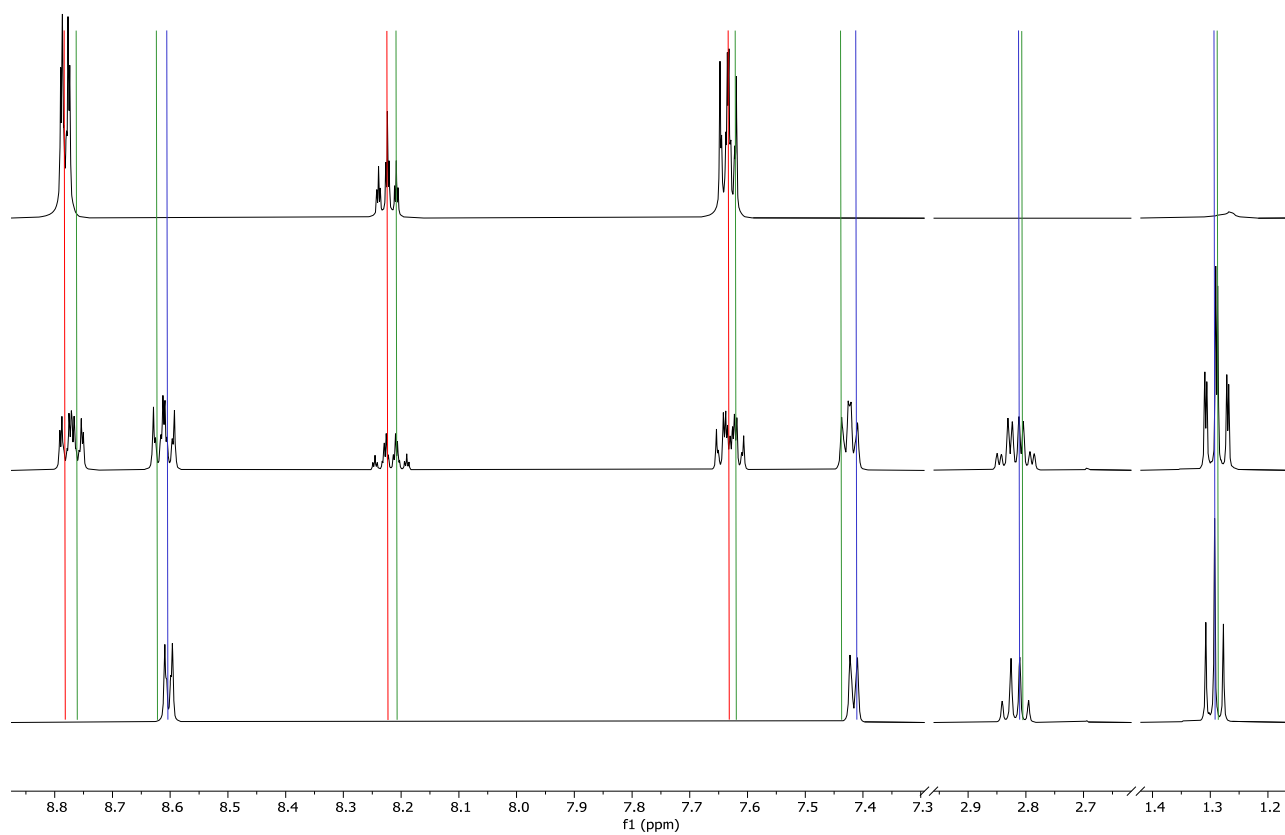
Figure S36: ^1H *(400 MHz, CD$_2$Cl$_2$, 298 K). Top: [bis(pyridine)iodine(I)]BF$_4$ ([(**1**)$_2$I]); Middle: A 1:1 mixture of [bis(4-(ethyl)pyridine)iodine(I)]BF$_4$ ([(**5**)$_2$I]) and [bis(pyridine)iodine(I)]BF$_4$ ([(**1**)$_2$I]); Bottom: [bis(pyridine)iodine(I)]BF$_4$ ([(**5**)$_2$I]). Selected regions are enlarged to demonstrate the doubling of the pyridine NMR signals. Coloured lines (red and blue) indicate the position of complexes [(**1**)$_2$I] (red) and [(**5**)$_2$I] (blue) while the remaining signals are attributed to [(**1**)$_1$(**5**)$_1$I] (green).*
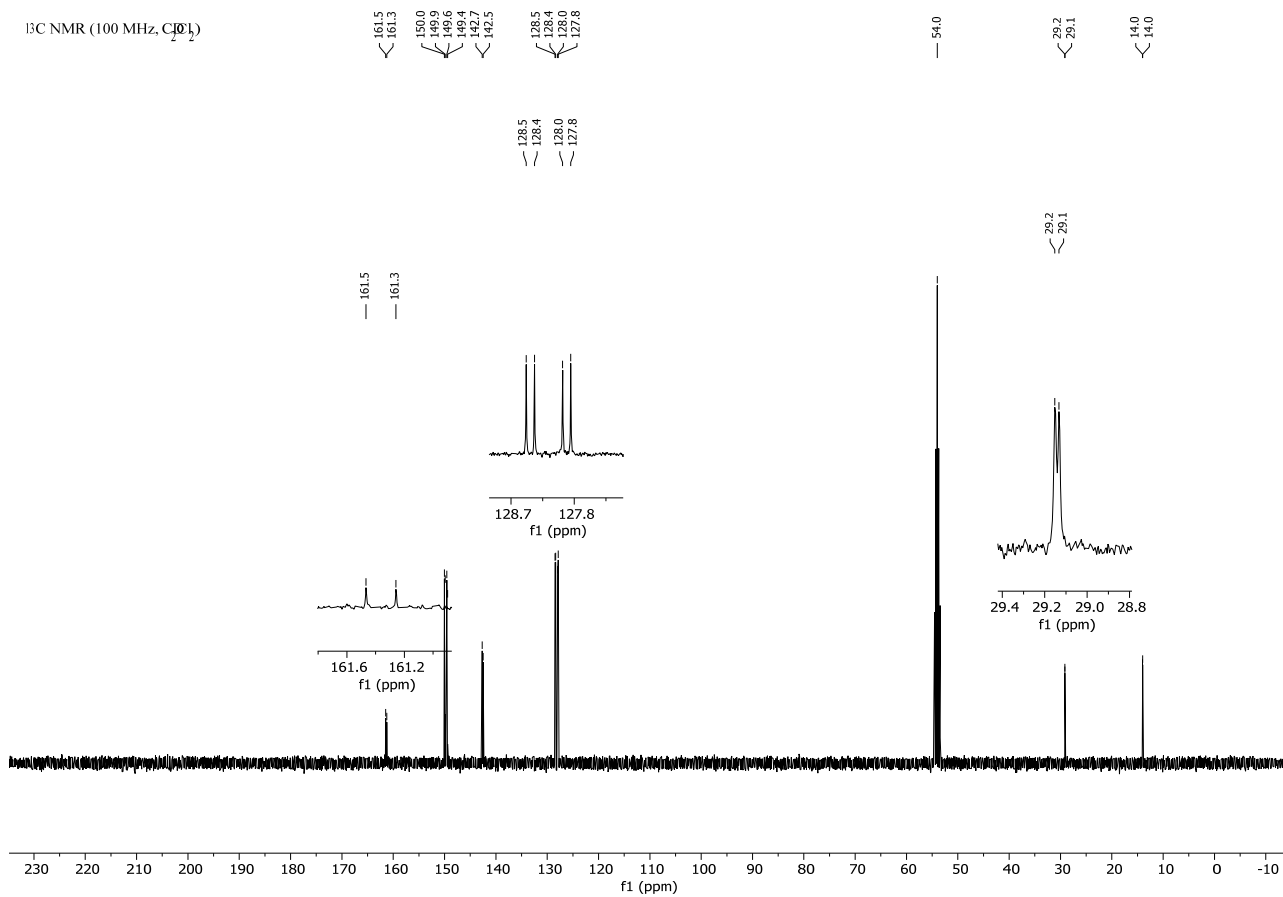
*Figure S37: ^{13}C (100 MHz, CD$_2$Cl$_2$, 298 K) of a 1:1 mixture of [bis(4-(ethyl)pyridine)iodine(I)]BF$_4$ ([**(5)$_2$I**]) and [bis(pyridine)iodine(I)]BF$_4$ ([**(1)$_2$I**]). Selected regions are enlarged to demonstrate the doubling of the pyridines NMR signals.*
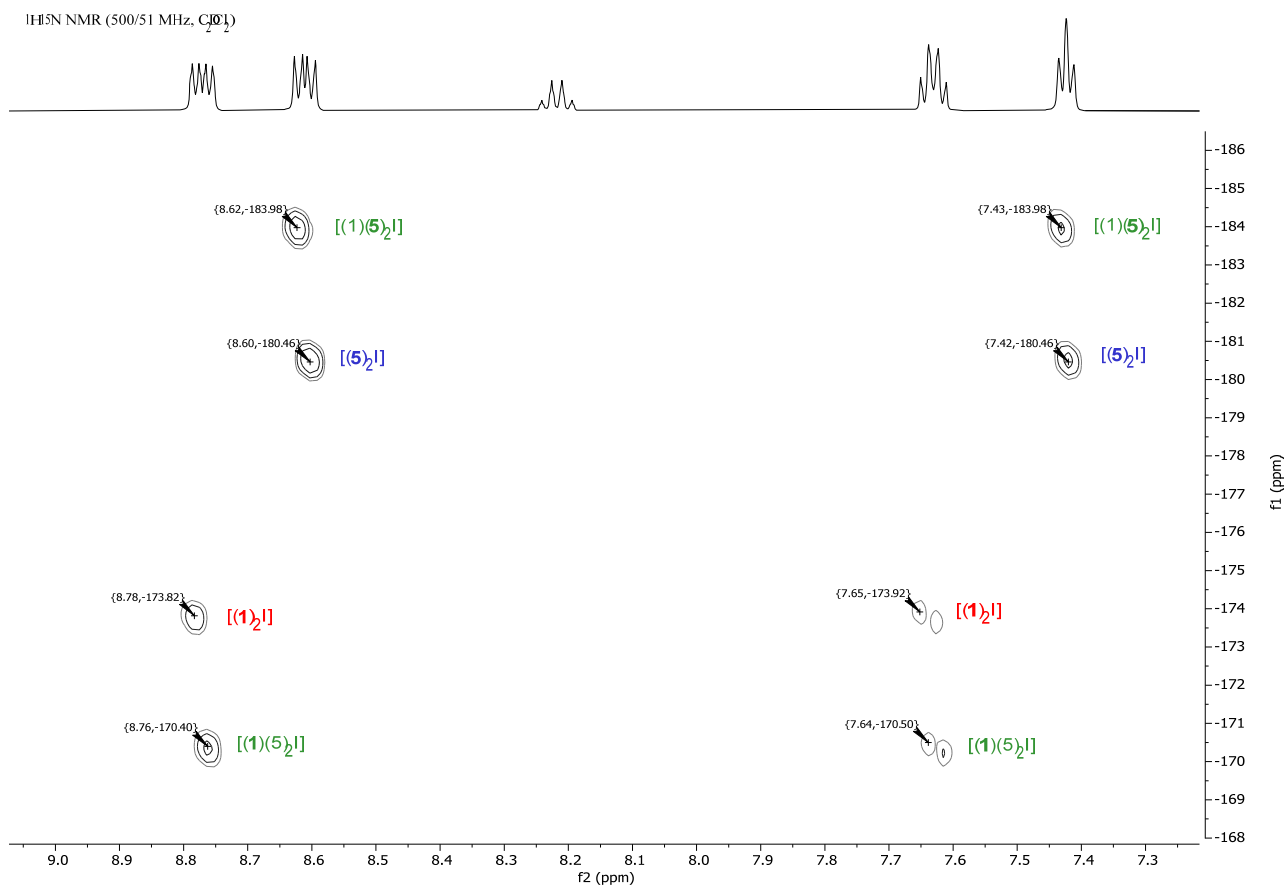
Figure S38: $^1H^{15}N$ HMBC (500/51 MHz, CD_2Cl_2, 298 K) of a 1:1 mixture of [bis(4-(ethyl)pyridine)iodine(I)]BF_4 ([(**5**)$_2$I]) and [bis(pyridine)iodine(I)]BF_4 ([(**1**)$_2$I]). It is evident that each multiplet observed in the ^1H NMR spectrum consists of the resonances of two different compounds.

4. References

1. D. von der Heiden, S. Bozkus, M. Klussmann and M. Breugst, *J. Org. Chem.*, 2017, **82**, 4037.
2. A.-C. C. Carlsson, K. Mehmeti, M. Uhrbom, A. Karim, M. Bedin, R. Puttreddy, R. Kleinmaier, A. A. Neverov, B. Nekoueishahraki, J. Gräfenstein, K. Rissanen and M. Erdélyi, *J. Am. Chem. Soc.*, 2016, **138**, 9853.
3. J. S. Ward, G. Fiorini, A. Frontera and K. Rissanen, *Chem. Commun.*, 2020, **56**, 8428.
4. T. D. W. Claridge, *High-Resolution NMR Techniques in Organic Chemistry*, Elsevier Science, 2016.
5. T. D. W. Claridge, in *Tetrahedron Organic Chemistry Series*, ed. T. D. W. Claridge, Elsevier, 2009, vol. 27.
6. H. Günther, in *NMR Spectroscopy - Basic Principles, Concepts, and Applications in Chemistry*, John Wiley & Sons Ltd, West Sussex, England, 2nd edn., 1995, ch. 9, pp. 353.
7. M. Bedin, A. Karim, M. Reitti, A.-C. C. Carlsson, F. Topic, M. Cetina, F. Pan, V. Havel, F. Al-Ameri, V. Sindelar, K. Rissanen, J. Grafenstein and M. Erdelyi, *Chemical Science*, 2015, DOI: 10.1039/C5SC01053E.
8. H. Andersson, A.-C. C. Carlsson, B. Nekoueishahraki, U. Brath and M. Erdélyi, in *Annual Reports on NMR Spectroscopy*, ed. G. A. Webb, Academic Press, 2015, vol. 86, pp. 73.

9. S. Lindblad, K. Mehmeti, A. X. Veiga, B. Nekoueishahraki, J. Gräfenstein and M. Erdélyi, *J. Am. Chem. Soc.*, 2018, **140**, 13503.